Master Thesis College of Human Ecology

Preparation of breathable superhydrophobic PU/SNPs hybrid nanowebs by electrospinning

- 투습가능한 초소수성 폴리우레탄/실리카 나노입자 하이브리드 전기방사 나노웹 개발-

August, 2014

Department of Textiles, Merchandising, and Fashion Design

The Graduate School of Seoul National University

JIN SHAO HUA

김소화

Preparation of superhydrophobic breathable PU/SNPs hybrid nanowebs by electrospinning

지도 교수 박정희

이 논문을 생활과학석사 학위논문으로 제출함
2014년 06월

서울대학교 대학원
의류학과
김소화

김소화의 생활대학석사 학위논문을 인준함
2014년 07월

위 원 장 _____ (인)

부위원장 _____ (인)

위 원 _____ (인)

ABSTRACT

Shaohua Jin

Department of Textile, Merchandising, and Fashion Design

The Graduate School

Seoul National University

Non-fluorinated polyurethane (PU)/SiO_2-nanoparticles (SNPs) composite nanowebs with superhydrophobic and breathable properties were prepared by electrospinning, using n-dodecyltrimethoxysilane (DTMS) as water repellent chemicals. The fiber morphology was examined by field emission scanning electron microscopy. The average fiber diameter was about 600-800nm with 1-6wt % SNPs, and they were observed spread on all of fiber surfaces.

The combination of the hierarchical surface roughness of PU/ SNPs nanowebs yielded a stable Superhydrophobicity with water contact angles as high as 159° and shedding angle as low as 5° by electrospinning and chemical vapor deposition (CVD)-coating process. The water contact angle (WCA) of pure PU nanowebs and PU/SNPs nanowebs increased from 131° to 151°, which could be attributed to the increasing size of the fiber diameter leading to increased roughness of the membranes. Besides, adding SNPs had positive effects on porosity of nanowebs, and thus of can be regarded as super breathable nanowebs. The water vapor transmission rate test showed that the moisture permeability of PU/SNPs was the highest. After through the treatment of DTMS hydrophobic surface-modification, the air permeability and water vapor transmission of the PU-SNPs-CVD nanowebs decreased comparing with the PU-SNPs nanowebs.

Keyword: Superhydrophobicity, Breathability, Non-flouro materials, Electrospinning

Student ID: 2011-23009

CONTENTS

List of Figures

List of Schemes and Tables

I. Introduction

1. Purpose

Superhydrophobic surfaces with self-cleaning, water repellency, and antifouling properties have received considerable attention due to their various applications for last few years, Drops of water on superhydrophobic surfaces exhibit high contact angles (>150°) and roll off at slight inclination (<10°)[1-5]. Polyurethane (PU) is one of the most important classes of polymer with elasticity, which imparts an elastic recovery property to the textile. Polyurethane is a thermoplastic elastomer composed of hard segments (diisocyanate) and soft segments (polyether). The carbamate groups in hard segments and the ether groups in soft segments provide comparable hydrophilicity, thus leading to high surface energy [6]. Various inorganic nanoparticles have been examined in order to improve surface roughness and superhydrophobicity by comporting nanoparticles on the polyurethane surfaces [7-20]. So as to reduce the surface energy of the nanoweb, fluorinated materials were employed to coating or polymerization [21, 22]. However, the organic-modified surfaces require extra organic reaction on nanoparticles and can be difficult to control the surface characteristics [23]. Also, fluoro-materials are expensive and thus limited their commercial applications [24, 25]. Electrospinning has become a popular method to generate continuous fibers with micro-nanometer diameters from a variety of polymeric materials [21, 22, 26-45].

The superhydrophobicity of a surface could be improved by texturing with multiple scaled roughness, and nanoparticles are widely used to create functional

nanoweb with nano-micro structures to improve the substrate property. In this paper, an electrospun fibrous nanoweb of non-fluoro polyurethane with superhydrophobicity and moisture permeability was prepared, wherein tetraethyl oxysilane (TEOS) made terminal alkyl group segment with polyurethane [46-49], and combined with silica nanoparticles. The addition of silica nanoparticles enabled the fibrous web surface to exhibit multi-level rough structures. So as to reduce the surface energy of the nanoweb, n-dodecyltrimethoxysilane (DTMS) was employed to process chemical vapor deposition (CVD)-coating [50]. Surface morphologies, surface chemical compositions, wettability, pore distributions and transport properties of fibrous nanoweb with different PU / SNPs constituents were researched.

2. Theoretical background

2.1 Superhydrophobicity

A variety of natural superhydrophobic bio-surfaces have drawn intensive attention from scholars, wherein lotus-effect was the most-watched focus. The superhydrophobicity of the lotus leaf is shown in Figure1-a, and 1-b. The water droplets on it maintain their dripping statuses. Moreover, the droplets are difficult to stay steadily on the lotus leaf, thus just a bit of tilt and vibration, they will instantly slip down. The lotus leaf surface has self-cleaning function and strong super-hydrophobic effect, where the static contact angle is 160.4 ± 0.7°, and the shedding angle is 1.7° This unique properties make it easy to take away the contaminants, that is what we call ‘ lotus effect.’

By the mid 1990’s, after researching into hundreds of plant leaves, the biologists Barthlott and Neihuis concluded that the self-cleaning characteristic was resulted from the joint action of the micron-scale mastoids (Figure 1-c) and hydrophobic waxiness[51, 52]. Cao et al.[53] reported improved view of Barthlott and Neihuis. They considered that the roughness of the lotus leaf surface was not just resulted from the action of the microstructures, actually, there existed nanostructures on its interfacial mastoids of micron size, and such combination of micro-nanostructures served as the root cause of the superhydrophobic surface. The SEM photograph of the mastoids on the lotus leaf surface is shown in Figure1-d, each of which was composed of nanostructure branches with average diameter of 120-130nm.

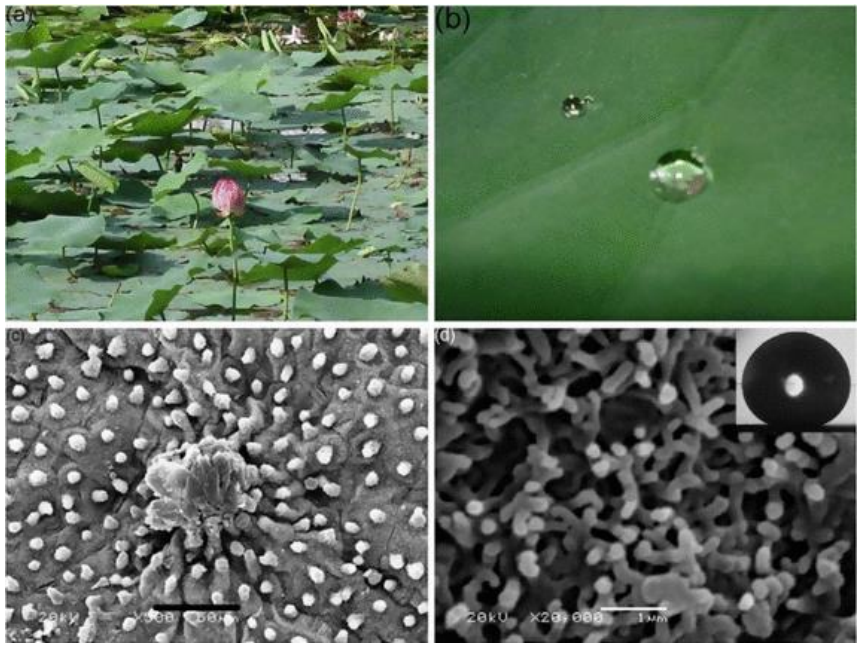

Figure 1(a). The photos of some lotus leaf (b) a water droplet on a lotus leaf (c and d) SEM image of lotus leaves with different magnifications, (c). The inset of (d) is a water contact angle on a lotus leaf, with a value of 161°±2°.

2.2. Approaches to preparing surface structures for superhydrophobic surfaces

There are numerous approaches to prepare superhydrophobic surfaces, whose essences are mostly derived from the bionic principle of superhydrophobic surfaces in nature. Jiang et al. [54] to prepare rough structure on the material surface; (2) to graft reagent with low surface energy on the rough surface. Based on the two basic principles, a large number of methods are employed to construct superhydrophobic surfaces, with the most common means: solution immersion method, multi-layer

assembly method, chemical deposition method, template approach and sol-gel method, etc.

2.2.1. Solution immersion method

Among all the methods, solution immersion is the simplest. During solution immersion process, a thin film is deposited on substrates. Early solution immersion method used to achieve the super-hydrophobic surface preparation through two steps; first, construct rough structure on the material surface; second, graft hydrophobic reagent on the rough surface. Cao et al. [55] report a solution immersion method for the preparation of superhydrophobic material, where the surface roughening and grafting were completed within one step: they placed a smooth copper sheet in fluoroalkylsilane solution, after the immersion, whose contact angle was tested to be 151° (as shown in Figure2).

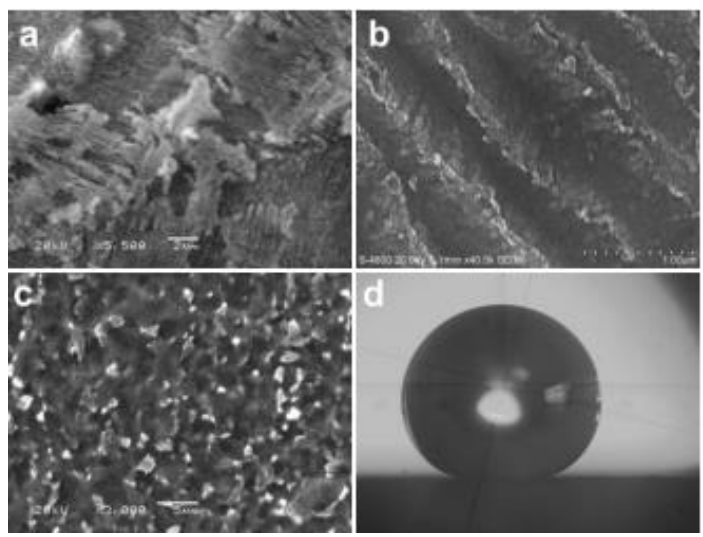

Figure 2. SEM images at a) low and b) high magnifications of the etched copper alloy treated with fluoroalkylsilane, the scale bar represents 20 μLand 1μL, respectively. c) SEM image of the etched

titanium alloy treated with fluoroalkylsilane, the scale bar represents 5 lm. d) Profile of a water droplet on the superhydrophobic titanium alloy surface having a CA of 151°±1°.

2.2.2. Layer-by-layer self-assembly process

Self-assembly is a process consists of spontaneous and uninstructed structural reorganization that forms from a disordered system. Such processes are reversible and held together by non-covalent intermolecular forces. The use of the LBL technique for constructing superhydrophobic coatings from poly(acrylic acid)(PAA) and polyethylene mine (PEI), especially using Ag+ to enhance the exponential growth of the PEI/PAA multi-layers has been explored[3]. It was found that the addition of Ag+ can significantly improve the surface roughness as shown in Figure 3. On such surface, a high contact angle of 172° can be achieved after surface fluorination by (tridecafluoroctyl) triethoxysilane.

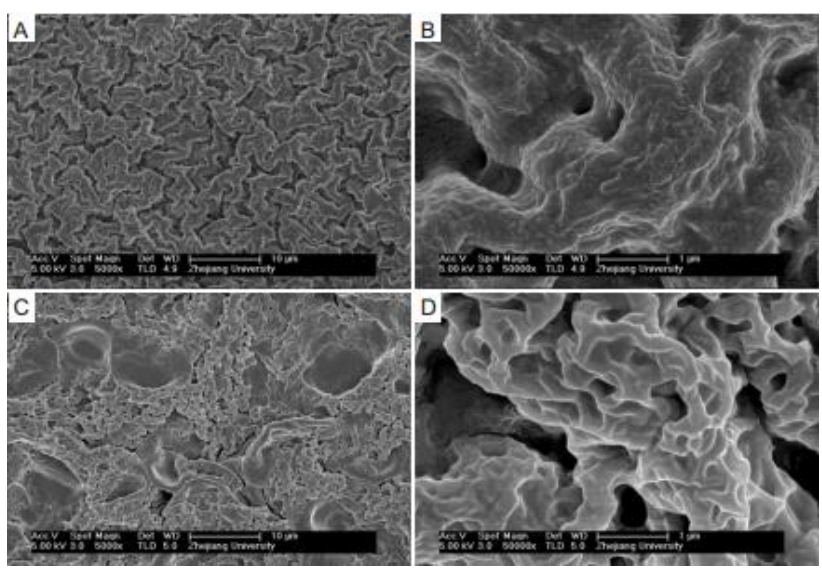

Figure 3. SEM images of (PAA/PEI) 7.5 films (A, B) and (PAA/PEI-Ag+) 7.5 films (C, D).

2.2.3. Chemical deposition approach

Chemical deposition is typically accompanied with some chemical reactions, during which the product will be deposited on substrate. This technique is generally used for the generation of inorganic crystal nanoweb, such as zinc sulfide, copper serenade, indium sulfide, and cadmium sulfide, etc. Chemical deposition methods could be classified into electrochemical deposition, chemical bath deposition (CBD) and chemical vapor deposition (CVD) [50]. The electrochemical formation of highly porous CuTCNQ (TCNQ=7,7,8,8 tetracyanoquinodimethane) and $CuTCNQF_4$ ($TCNQF_4$ = 2, 3, 6-tetrafluoro-7, 7, 8, 8 tetracyanoquinodimethane) materials was undertaken via the spontaneous redox reaction between a porous copper template, using a hydrogen bubbling template technique and acetonitrile solution containing TCNQ or $TCNQF_4$, as shown in Figure 4. This combination of micro and nano roughness was found to be extremely beneficial for anti-wetting properties where superhydrophobic materials with contact angles as high as 177° were created.

Figure 4. FE-SEM image of porous copper electrodeposited on to copper foil and contact angle.

2.2.4. Template approach

Template approach is typically employed for the preparation of polymer-based super-hydrophobic surface, with the steps as follows: first, select a motherboard with certain surface characteristic and copy the surface, subsequently, take out the reproduction or dissolve the template. The template used could be a plant in nature, a commercial inorganic web, or an etched motherboard. Lee et al. [56]reported that using AAO Template, PS superhydrophobic surfaces with well-defined nanostructures could be fabricated as shown in Figure 5. Studies on the present biomimetic surfaces revealed that the wetting property of the nanostructured surface of a given chemical composition could be systematically controlled by rendering nanometer-scale roughness.

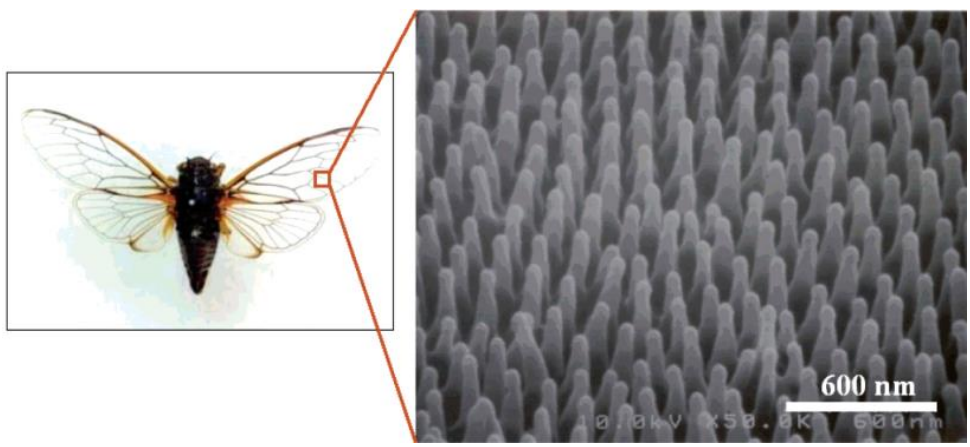

Figure 5. FE-SEM micrograph of the wing surface of C. orni with regularly aligned nanoposts.

2.2.5. Sol-gel method

Sol is commonly obtained by hydrolysis of the corresponding oxides in a solvent, and during the gel formation process, a large amount of solvent will fill in the grids to form some jelly-like substance. Silica Sol, typically prepared through

hydrolysis and condensation of TEOS, can either be directly used or used together with the silica nanoparticles. The surface property obtained can be varied depending on both the sol preparation process and the feature of the functional group on the sol surface. Tadanaga et al. [57] prepared Al_2O_3 web on the glass sheet through employment of the sol-gel method, whose surface roughness could achieve 20-50nm after roughening treatment by boiling water, and finally, the water contact angle reached up to 165° after modified with fluorinesilane.

2.2.6. Electrospinning method

Electrospinning is an effective way to form the web with three-dimensional network space structure, and the nanofibers materials have advantages of material diversity, high slenderness ratio, high porosity, high specific surface area, uniform structure and so on. It is obvious that the application of the electrospinning method could quickly prepare the micro-nano combined nanofibers with high surface roughness and composite structure.

Recently, Li et al. [58] prepared PS superhydrophobic fiber web with greatly improved mechanical properties (PS concentration of 30%, THF/DMF = 1/3), whose static contact angle could reach 154°, with fluctuated grooves on the surface, which proved extremely similar to the silver ragwort leaf in nature(as shown in Figure 6).

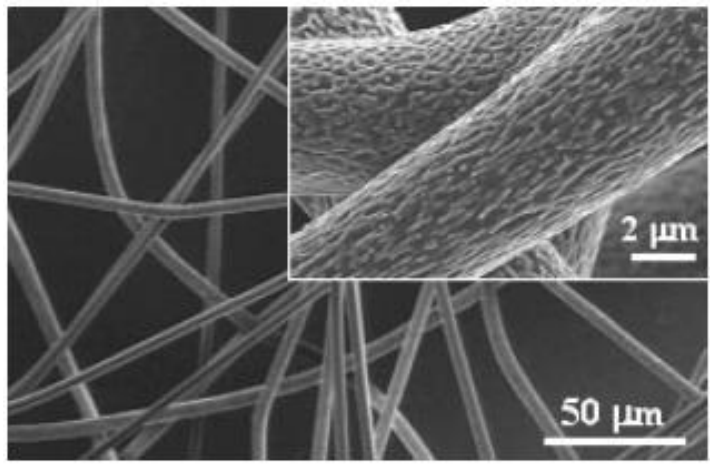

Figure 6. SEM images of the electrospun PS fibers formed from various weight ratios of THF/DMF in solvent: (1/3).

[1] introduction to electrospinning

In the electrospinning, high voltage is applied to the polymer solution or melt, which will firstly form Taylor conical liquid droplet through the spray-hole. After the tensile force generated by the high voltage electric field overcomes the surface tension of the droplet, the charged droplet will form a jet, which will get further stretched in the electric field, meanwhile, the solvent within the jet will continuously evaporate, and spirally reaches the receiver and solidifies to form a non-woven mats or fiber-like structure of other shape.

This technique was proposed as early as the 1930s. From 1934 to 1944, Formals'[59] applied for a series of patents and invented the experimental device for polymer fiber preparation by electrostatic force, wherein the natural polymer cellulose solution was introduced into the electric field, and fibers were obtained from the polymer solution between the electrodes with opposite charges. One electrode was connected to the collector, and the other to the solution. When the

polymer solution squirted from the metal spinneret with tiny holes, the solvent of the charged effluxion evaporated to become fibers under the electric field force, and be collected on the collector. Moreover, the desired voltage difference was determined by the properties of the spinning solution, such as molecular weight and viscosity. When the distance between the spinneret and the collector was relatively small, since the solvent did not completely evaporate, the spun fibers would adhere to the collecting device and also adhere to each other. Electrospinning can easily make the polymers into micro-size or even nanofibers.

Since 1990s, the electrospinning gradually earned more and more attention from scholars. Electrospinning serves as one of the most significant methods of producing nanofibers. Through electrospinning, any polymer with fiber-forming performance could be made into nanofibers. Currently, nanofibers have been successfully prepared from more than one hundred types of polymers and other types of materials. There are lots of methods available for the preparing superhydrophobic materials, and each has advantages and disadvantages. Compared with other methods, the electrospinning process, the only one capable of preparing polymer nanofibers directly and continuously, can prepare unique-structured fibers which could form particular network structure with super-high specific surface area and high porosity. Other principal advantages are relatively simple production process and equipment, and low cost. Additionally, the electrospinning technique applies to a wide range of raw materials, which may include most of the presently known soluble (fusible) polymers with a certain molecular weight, such as natural high polymers, compound polymers, nanoparticles, or drug delivery polymers and ceramics, etc. The electrospinning process is also highly controllable, and through the convenient control on the process parameters, fiber materials with different scales, patterns and usages could

be prepared.

[2] Basic principle of electrospinning

The research of Taylort [60], the first to propose the basic principle of the jet flow during the electrospinning process, demonstrated that solution with certain viscosity may be stretched in the capillary by the electric field force. When the voltage across the capillary rises, the liquid will become a cone, with the application point of the electric field force at the cone tip. The instant the potential reaches a critical value V_C, the cone angle will be 49.3 °, and then the charged cone is called 'Taylor cone'.

In a typical electrospinning experiment, when no or very small electric field force is applied, the high-polymer droplets are squeezed to the spinneret to form a charged cone, i.e. Taylor cone, when the surface tension plays a dominant role and the voltage continues to rise, until it reaches over the critical value Vc, the electrostatic repulsive force formed by the charges on the droplet surface will exceed its own surface tension and viscous force, and then the electric field force will overcome the surface tension and the viscous force of the solution to form charged liquid trickle at the top of the Taylor cone, which will run within the electric field and get further stretched, and meanwhile, the solvent will evaporate to become superfine fibers and deposit on the receiver, that is the fiber web. The process above could be divided into two stages:

A. Jet in the stable stage

After the electric field force overcomes the surface tension and the viscous force of the solution, the charged jet will spurt from Taylor cone into the electric field. In the initial stage, the electric field force plays a leading role, which will get

the charged jet to do an accelerating linear motion in the electric field.

B. Jet in the unstable stage

Unstable jet serves as the most crucial factor to obtain nanofibers. Electrospinning jets may exhibit one or a variety of unstable modes, depending on the basic parameters of jet velocity, radius and surface charge density, etc.

Furthermore, there are numerous influencing factors in the fiber preparation process, mainly some process parameters, such as solution properties, including viscosity, conductivity, elasticity and surface tension, etc.; control variables such as voltage, solution advancing speed, hydrostatic pressure in the capillary, potential of the capillary orifice, distance between the capillary orifice and the collector, etc.; ambient parameters such as air temperature and humidity.

The solution concentration has a significant influence on the morphology of the electrospun fibers, and too low or too high will bring difficulties to the spinning process. Generally, if the polymer concentration is too low, more bead-on-string fibers will be obtained on the receiver, not fibers with normal morphology. Otherwise, if the polymer concentration is too high, due to too large viscosity, the flow rate of the spinning solution can’t be continually and precisely controlled. Then the spinning is rather difficult, or ever impossible.

Receiving distance refers to the distance between the needle tip and the collector, TCD for short. Too large TCD will weaken the stretching action on the jet and thus affect the fiber molding due to the decrease in the electric field force; otherwise, if the TCD is too small, time for stretch and solidification decreased and the incomplete evaporation of the solvent may result in fiber crosslinking phenomenon.

During the electrospinning process, after being pushed out of the needle by the

injection pump, the droplets subjected to the tension of the electric field force will form fibers and continuously be deposited on the receiver. When other experimental parameters are fixed, the fiber would get thinner as the spinning voltage increased, however, when the spinning voltage increased to a certain critical value, the average fiber diameter will increase with the increasing spinning voltage.

The increase in the advancing speed of the injection pump could raise the electrospinning productivity, but not unlimited growth. After reaching a critical value, excessive solution being pushed out by the injection pump can’t solidify in time and will spatter. Worse still, so there is a blockage possibility for the nozzle, which will hence influence the continuity and efficiency of production.

2.3 Polyurethane

The polyurethane(PU) is one of the most important classes of polymeric materials with repeating structure of carbonate chain(in shown Figure7) [61]. The raw material of PU elastomer mainly comes from the following three kinds of substance: 1. polyhydric alcohols low polymer (Polyester and polyether etc.); 2．isocyanic acid (TDI、MD、PAPI etc.); 3. chain extender (MOCA etc.).

The molecular chain of PU generally consists of two parts. Bonart [62] first described the structure into soft segment and hard segment. PU can be considered as a segmented copolymer with soft segments and hard segments. Soft segment is made up of low polymer polyhydric alcohols (usually polyether, polyester or polyolefin glycol) and generally assumes the state of random coil. Its glass transition temperature is lower than room temperature and its chain segment is very soft, which contributes to the name of flexible segment (or soft segment). Hard segment is made up of polyisocyanates or its macromolecules chain extension (or hard segment). Owing to the incompatibility of forces, the two kinds of segments will experience microcosmic separation and form phase domain and micro phase domain. In 1996, Cooper S L et al. [63]first put forward the theory of micro phase separation according to the linear viscoelasticity of PU. There are many groups including carbamic acid ester, urea, ester and ether in PU which produce extensive hydrogen bonds, among which, the hydrogen bond produced by ammonia ester and urea bond contributes relatively much to the formation of hard segment bundles. The unique flexibility and wide range of physical properties of PU can be explained with two-phase morphology. The hard segment phase of PU serve as the enhancer, providing physical cross-linking to polyfunctional group, and the soft

segment matrixes are cross-linked by the hard segment phase areas. The excellent performances of PU are mainly due to the formation of micro-phase area, rather than simply the hydrogen bond between the hard segments and soft segments. Because of its unique chemical structure, it provides with the specialties of abrasion resistance, flexibility and chemical resistance as well as rich and smooth feel.

PU is a unique polymeric material with wide range of chemical and physical properties, which feature excellent properties like being anti-abrasion, anti-bending, anti-aging, highly adhesive, good cold resistant, breathable, wash available, inexpensive, and convenient to manufacture. Due to these characteristics, it is widely used in textile materials such as the coating of textiles, artificial leather and garment fabric, though defects such as poor hydrophobicity still exists. At present, the widespread method of preparing superhydrophobic PU is either PU fluorination or surface treatment with fluoride. Also, fluoro-materials are expensive and environmental polluting substances, thus limited its commercial application.

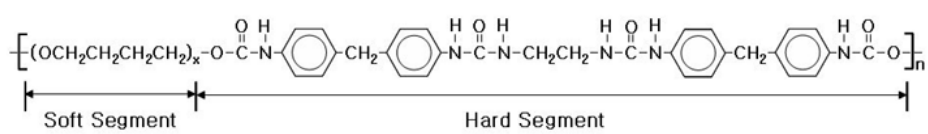

Figure 7. Illustration showing the chemical structure of Polyurethane.

2.4. Ormosils

During polyurethane modification emerge two problems about nanoparticles: one is their dispersion, and the other is their compatibility with polyurethane substrate. Although traditional nano-powder modifiers, such as micro-molecule coupling agent and surface active agent, can reduce the surface energy of nanoparticles, yet they are not able to entangle the molecular chain of polyurethane and achieve good compatibility for shorter molecular chain, thus leading to poor compatibility between the modified powder and the polyurethane substrate. For this reason, no evident effect is witnessed in polyurethane performance enhancement. On the other hand, the utilization of macromolecule modifier solved this problem. The active anchoring group on the macromolecule modifier can react with the surface active group of nano-powder. By this, the macromolecule modifier is secured on the surface of nanoparticles while the surface of nano-powder is wrapped around by the long flexible chain on the macromolecule modifier, thus achieving good compatibility between nanoparticles and polyurethane substrate.

Ormosils are organic-inorganic hybrid solids in which the organic component may be chemically bonded to a silica matrix. The structure of the silica network can be modified by the presence of organic groups [64].

With large specific surface and high surface energy, nanoparticles are extremely easy to form agglomerate. In addition, huge free energy difference between the substrate interfaces of inorganic nanoparticles and organic polymer as well as poor compatibility both lead to forming large amount of agglomerates of nanoparticles in the polymer substrate. As a result, voids occur in the interface and phase separation appears. Currently, these two are the most crucial problems which have to be solved in making polymer or nanoparticle composites. Thus, surface

energy of the nanoparticles has to be reduced to make them evenly dispersed and show good compatibility in the polyurethane substrate.

The simplest Ormosils are those formed from precursor such as $RSi(OCH_3)_3$ where R is an organic terminal group which does not form a bridge in the three-dimensional gel network (Scheme 1 (1-A)) [65]. Alternatively, one can start with $R_2Si\ (OCH_3)_2$ and mix in TEOS. Thus, the subsequent 3D SiO_2 network will have a controllable number of terminal oxygen. Such precursors with more complex R groups are exemplified by the polyurethane shown in Figure 8(1-B). The organic group is now optically active. Gels can be formed by mixing PU with TEOS [23].

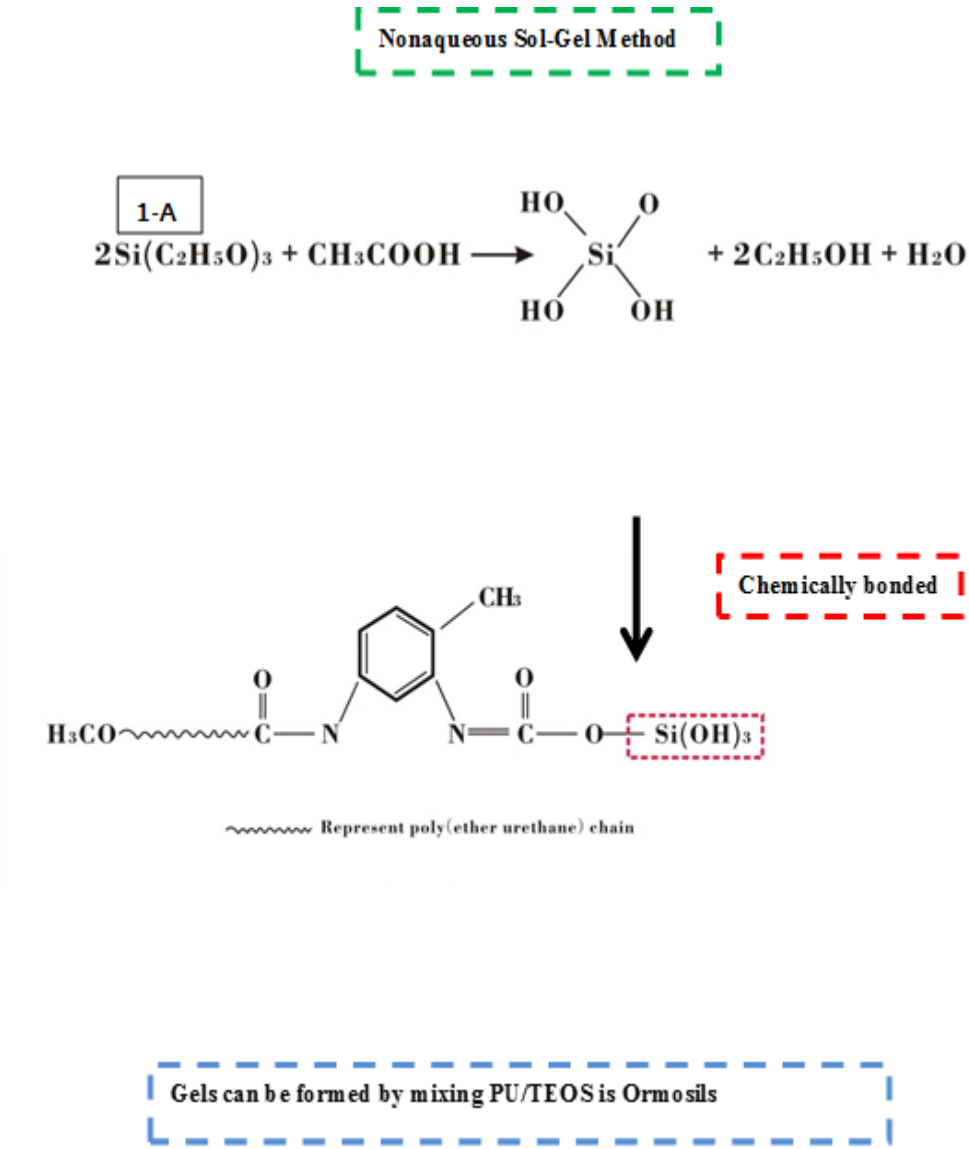

Scheme 1. The structure of Ormosils where the polyurethane and TEOS constituents are chemically bonded.

II. Experimental

1. Materials

All reagents were used without further purification. Polyurethane (PU) (pellethane 2103-80AE) was obtained from Lubrozil (USA). It is a polyester type with average Mw of 80,000 (shown in table 1) and hydrophobic silica nanoparticles (SNPs) (AEROSIL® R 972, Evonik, USA). Dimethylformamide (>98%) and tetrahydrofuran (>98%) is solvent from DAEJUNG (KOREA). Tetraethoxysilane (>98%) is silicone coupling agent from DAEJUNG (KOREA). n-dodecyltrimethoxysilane (DTMS) (>98%) was obtained superhydrophobic surface by chemical vapor deposition from the Aldrich Chemical Co. (USA).

Table 1. Specification of polyurethane.

Materials	Mw	Tm	Tg	Density (at 25℃)
Polyurethane	**80,000**	**182℃-210℃**	**-40℃**	**1.13g/mL**

2. Web preparation

Detailed process is shown in Fig 8:

Step.1

PU pellets were poured into the solvent with a volume ratio of DMF and THF

of 4:1，they were mixed uniformly with a magnetic stirring apparatus and an ultrasonic stirrer.

Step.2

Meanwhile the mixed solution of TEOS and acetic acid were stirred by magnetic stirring apparatus for 10 minutes for non-hydrolytic sol-gel. Finally silica particles with the diameter of 16nm were added to get silica gelation.

Step.3

Two kinds of solution were stirred again with the rotate speed of 300rpm/min for 24 hours. The electro spinning coefficients vary by viscosities of various solutions. The fiber membranes were obtained in the vacuum oven at 25℃ for 24 hours so as to volatilize all of the solvent residual in fiber membranes. At last, DTMS was coated on electrospun nanoweb surface to get superhydrophobic breathable membranes (shown in Figure 8).

Step.4

In the research, the PU/SNP_5-CVD nanoweb laminate polyester was prepared by electrospinning and chemical vapor deposition treatment on the polyester fabric, and the electrospinning parameters remained same.

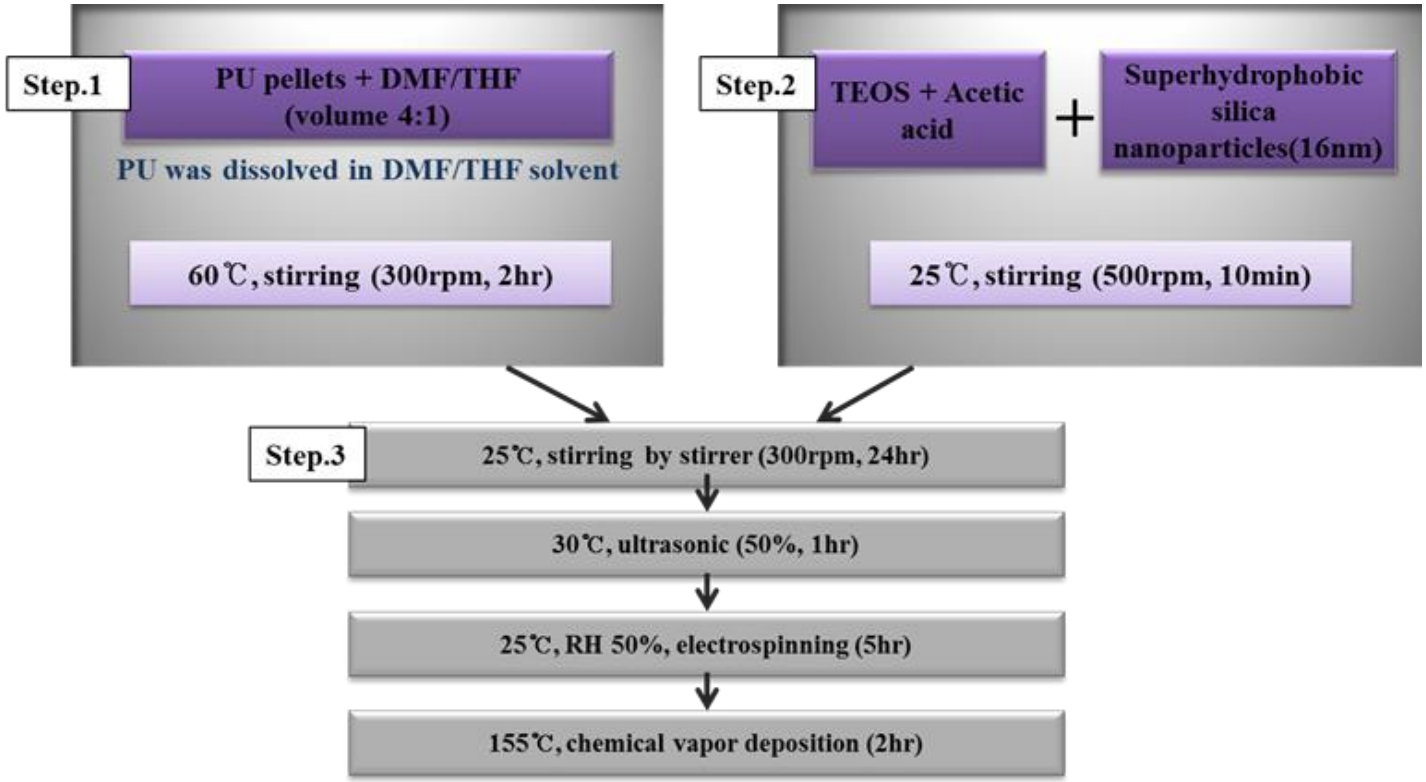

Figure 8. Image of process the PU/SNPs nanoweb by electrospinning

2.1 Electrospinning process

Since that we are trying to spin with organics and organics-inorganics, two kinds of solution with different viscosities, to get a similar fiber diameter, different spinning parameters should be set. In addition, the critical point in getting the same fiber diameter lies in that the surface roughness of pure PU fiber membranes is similar to that of fiber membranes added with SNPs.

Using the receiver with a rotary drum with laterally reciprocating movement could improve the receiving homogeneity of the fiber web. The device shown in Figure 9 is one of the production devices relatively in line with the development trend. The injection pump is mounted on the metal base and can move with it. The metal rolling drum connected to the adjustable varying-speed motor is grounded during the test; the linear speed of the lateral shifter and the rotational speed of the metal drum can be controlled. Table 2 was showed variation nanoweb of electro-spun condition. All the samples were dried in a vacuum oven at 60℃for 24 h before testing.

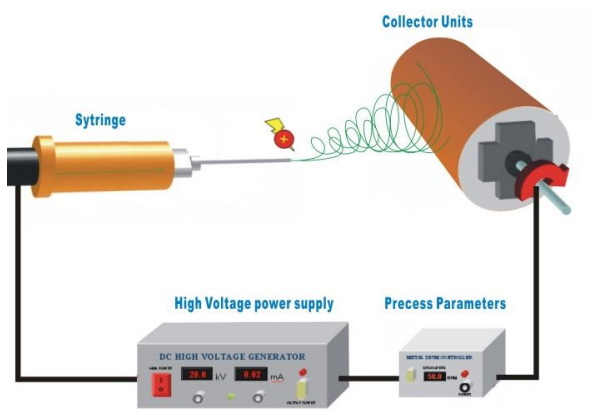

Figure 9. A scheme of basic electrospinning set up.

Table 2. Electrospinning condition.

	RH	Temperature	Distance	Feed rate	Voltage
PU	50±5%	25℃	14cm	1㎖/h	14kV
PU-SNPs	50±5%	25℃	20cm	0.2㎖/h	18kV

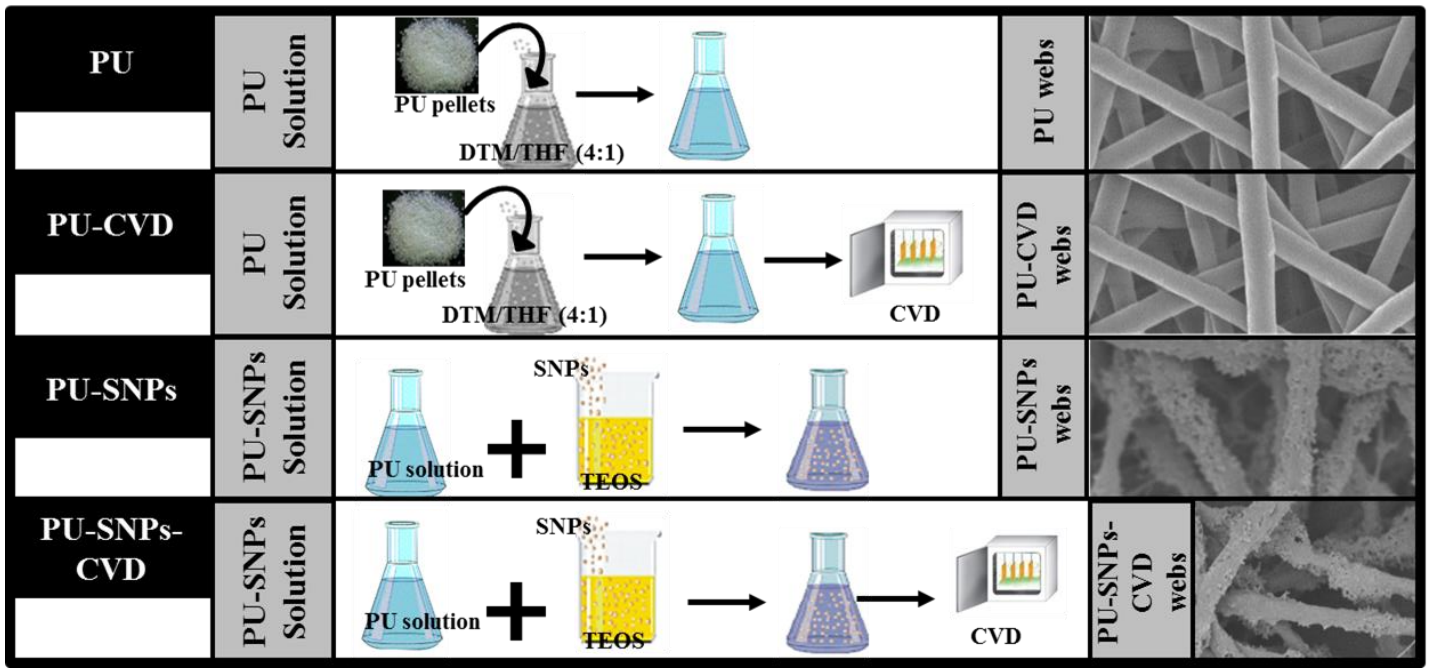

2.2. Preparation of PU web

The solvent were poured into a reagent bottle with magnetic stirring rotor, and the PU pellets were dispersed evenly. Afterwards, we placed the bottle on the magnetic stirring apparatus with a speed of 300rpm in constant temperature for several hours. The electrospinningability requirements were accomplished when we got colorless and transparent solution.

PU solutions concentrations of 10 wt%, 11 wt%, 12 wt%, 13 wt%, and 14wt% were prepared by using DMF/THF mixture with a volume ratio of 4:1[61].

Electrospinning process was conducted at 25±2℃ and 40±5% RH (Relative Humidity). The solution was placed into a 10-mL syringe capped with a 25G blunt and needle. A rectangular aluminum foil was bundled around a grounded metal rotary drum (rotating rate, 100 rpm), which was placed 14 cm from the tip of the needle as a rotating collector. The voltage was kept at 14 kV, and the solution flow rate was 1 mL/hr.

2.3. Preparation of PU-SNPs web

To achieve successful electrospinning, it is necessary to ensure appropriate concentration of polymer solution and particles. On the basis of trial and error, in the spinnability, we have determined the details of solution preparation of PU-SNPs fiber membranes. Meanwhile, we identified the parameter of PU-SNPs nanoweb preparation as follows: the PU concentration is 8.2 wt% with DMF/THF as the solvent. The mass fraction of SNPs is 1wt%-6wt% in the PU/SNPs solution.

First, TEOS/acetic acid, silica nanoparticles and the solvent DMF/THF were prepared according to the requirements of concentration of PU-SNPs solution and

solvent system. Then the solvent was poured into a reagent bottle with magnetic stirring rotor, and then the PU pellets were dispersed evenly. Finally we poured the silica nanoparticles in evenly dispersed PU solution; we covered the cap and sealed the bottle quickly. Afterwards, we placed the bottle on the magnetic stirring apparatus with a speed of 300rpm in constant temperature for several hours until the silica nanoparticles are completely and evenly dispersed in the PU solution. The spin ability requirement was accomplished when we got colorless and transparent solution.

The PU-SNPs nanoweb was prepared by accomplishing three-steps. First, sol–gel reaction was carried out with the composition of TEOS/acetic acid (1:2/w:w) to form the primary particles. Second, silica gelation were produced by adding AEROSIL® R 972 in the first solution, the silica gelation was composited with 8.2wt% PU solution and followed by electrospinning and dried to form the PU-SNPs nanoweb. SNPs concentrations of 1 wt%, 2 wt%, 3 wt%, 4 wt%, 5 wt%, and 6wt% were prepared by using polyurethane solution mixture with TEOS/acetic acid of 1:2(w/w).

Electrospinning process was conducted at 25±2℃ and 40±5% RH. The collector was placed 18 cm from the tip of the needle is 18 cm. The voltage was kept at 14 kV, and the solution flow rate was 0.2 mL/hr.

2.4. Preparation of PU-SNPs-CVD nanoweb

Chemical vapor deposition (CVD) is a kind of process technology with which we enable the physical vapor deposition of reactive materials in gaseous state, which generate solid matters depositing in the heated solid matrix surface and then get solid materials. Chemical vapor deposition is a kind of vapor phase growth

method to prepare materials. We utilized this process technology to place one or more kinds of compound with membranes elements and gases with simple substance into the reaction chamber with base materials and get solid membranes depositing in matrix surface in virtue of chemical vapor reaction.

In the studies, PU-SNPs were cured at 150℃ for 3h for DTMS chemical vapor deposition coating in an oven[66]. The chemical structure of the PU/SNPs nanoweb was shown in Scheme 2, the PU/SNPs nanoweb were electrospun at first (a)[67, 68], the Si–OH groups in DTMS could react with both the SiO_2 nanoparticles and the fiber substrate since there are abundant OH groups on the SiO_2 and PU fiber surfaces. As a result, the SiO_2 nanoparticles and the fiber substrate were tightly bound with each other (c).

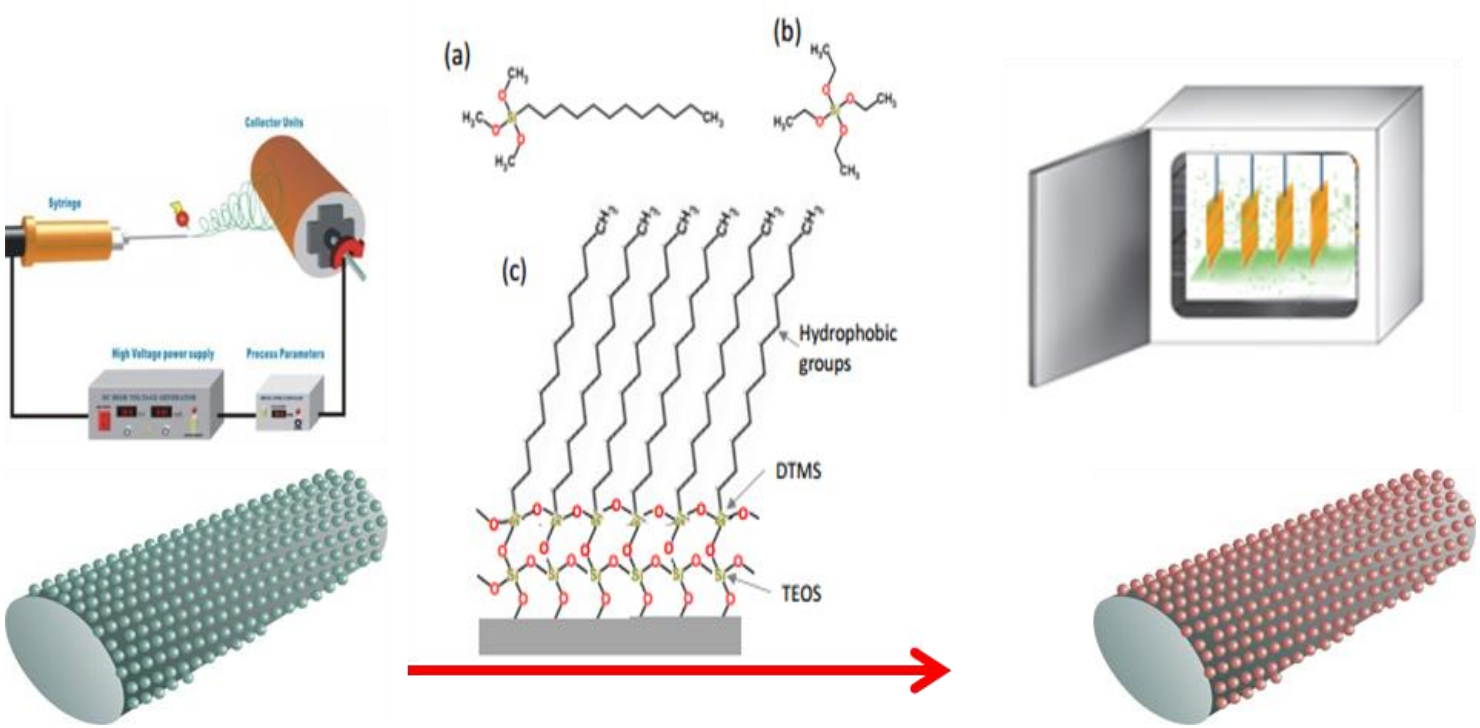

Sheme 2. Chemical structures of DTMS (a) and TEOS (b) and a proposed schematic diagram of sol–gel films formed on the substrate (polyurethane/silica nanoparticles webs) (c).

3. Characterization

3.1. Observation of surface morphology

Morphology of the collected fibers was observed by the Field Emission Scanning Electron Microscope (FE-SEM, JEOL, JSM-7600F. USA) with an acceleration voltage of 120 kV. whereas verification of the PU/SiO_2 structure was conducted by Energy-Filtering Transmission Electron Microscope（EF-TEM）(LIBRA 120, Carl Zeiss, Germany) with an accelerating voltage of 120 kV. The samples for SEM observation were sputter coated with gold. Fiber diameters of the electrospun fibers were measured with the image visualization software Image J (National Institutes of Health, USA). Averaged fiber diameters were determined from about 600–800 measurements upon a typical SEM image.

3.2. Mechanical property measurement

Tensile experiment

There are several main evaluation indicators for tensile test, including tensile strength, elongation and elasticity modulus. We only carried on research into the tensile strength and elongation in this study.

Tensile Strength

The original cross profile (F) in the stretching position (F refers to the product of initial breadth and thickness of the sample) divided by the maximum force (S) suffered by materials during the stretching process is tensile strength (σ), commonly known as breaking stress. The computational formula is:

$$\sigma=\frac{F}{S} \quad (1)$$

Elongation

When the maximum transformation （L-L_0）from the beginning of the experiment till the breakage was divided by the preliminary gauge length(L_0) and then it was multiplied by the percentage, you can work out the specific value——elongation (2) , known as elongation at break.

$$\varepsilon=\frac{L-L_0}{L_0}\times 100\% \quad (2)$$

All of the tensile tests in this text utilized Instron-5543-type electronic single-fiber strength tester. We conducted the electrospinning fiber membrane strength test according to ASTM D 5035. The sample was cut into one with a length of 10mm and a breadth of 40mm. The distance was 50mm and the stretching velocity was 10mm/min. we tested 5 times for each sample and documented the load and elongation curve until the fiber membrane broke. We used the averages of measured values such as breaking strength and calculated the variable coefficient of all indicators.

3.3 FTIR analysis

Fourier transform infrared spectroscopy (FTIR; Nicolet 6700, Thermo Scientific, USA) was used to identify the change of functional groups of different blend and solution formulas. The electrospun nanoweb collected was analyzed in

absorbance mode in the range of 600–4000 cm^{-1}. Silicon dioxide nanoparticle distribution on the surface of PU/SiO_2 fibers was investigated by an energy-dispersive spectroscopy (EDS; Nicolet 6700, Thermo Scientific, USA)

3.4 Evaluation of Surface wettability property

3.4.1Static contact angle

The static water contact angle (WCA) was determined by using the contact angle measurement device (Theta Lite, Attention, KSV Instrument, and Finland). At 23 ± 5℃, a 4μl droplet of deionized water was placed on five different positions on the sample surface, and the angles of drops on the specimens were determined. The static contact angle values for the sample reported were the average of five measurements.

3.4.2 Shedding angle

Water shedding angle (WSA) of various samples was measured by the method of Zimmermann et al. [69] after releasing a drop of water (12±0.5 μl) in a height of 1cm, the minimum angle of inclination at which the drop completely rolls off the surface was determined. The shedding angle values for the sample reported were the average of five measurements.

3.5 Transport property measurement

3.5.1 Air permeability

An 1100-AEHXL capillary flow porosity (Porous Media Inc., Ithaca, NY) was used in this study to nanoweb structure by Frazier air permeability testing instrument. The measurement was carried out according to the ASTM D737-04 standard method, with 1.4 mm orifice, 2.75 square inch test area, at 30 inch mercury pressure, 21 ℃, 65 % RH.

3.5.2 Water vapor transmission (WVT)

① ASTM E96: KS K0594 (Calcium chloride upright cup method)

The WVT across the material was measured by ISO 15496. The specially designed cup was filled with calcium chloride and the specimen membrane was fixed onto its opening. The cup mouth defined the area of membrane exposed to the environment. Then the assembly was hanged up-side-down in an thermo-hygrostat at 40℃ with a constant relative humidity of 90 %. After 1 h, the evaporation of water through the membrane was monitored by the weight change of the cup and the WVT was calculated by the following equation (3).

$$\mathbf{WVT} = \frac{G}{tA} \mathbf{x\,24} \tag{3}$$

G: weight change, grains (from the straight line) (g)

T: time during which *G* occurred [70],

A: test area (cup mouth area) (m^2)

WVTR: rate of water vapor transmission (g/m^2*24hr).

III. Results and discussion

1.Surface morphology

1.1 PU nanoweb

Polyurethane is a type of polymer composed of the hard segment (isocyanate) and the soft segment (polyester or polyether). And THF serves as the excellent solvent for the soft segment, so does DMF for the hard segment; therefore, the DMF/THF mixed solvent was employed as the solvent for PU in this study. PU solutions with different concentrations were prepared to obtain fibers with various diameters, wherein the mass fractions were 10 wt%, 11 wt%, 12 wt%, 13 wt% and 14 wt%, respectively, with variation in the morphology of different concentrations of PU solution by electrospinning was shown in Fig10.

It has been demonstrated through a great number of researches that in case of relatively low concentration and viscosity of the electrospinning solution, only the polymer beads could be obtained, that is because the liquid jet flow will be tensioned in the electrostatic field, the molecular chains without or with insufficient entanglement will fracture, for they are unable to effectively resist the external force. Meanwhile, they have tendencies to shrink under the viscoelasticity of the polymer molecular chains, which will result in molecular chain agglomerations and eventually form polymer beads. When the concentration and viscosity of the solution are above certain critical values, the entanglement degree between molecular chains will increase, thus the solution jet will suffer longer relaxation time under the electric field force, and the tangled molecular chains will be

oriented along the axial direction of the jet flow, which will effectively inhibit fractions of partial molecular chains among the jet, as a consequence, continuous electrospun fiber structures could be eventually obtained. An increase in the solution concentration could decrease the surface tension of the solution to some extent, which contributes to the formation of continuous and uniform fibers.

The FE-SEM images of the electrospun nanoweb of polyurethane under different concentrations were shown in Fig 10, which indicated the randomly-oriented 3D non-woven structures. Concretely, the diameter of PU-10 nanofibers are not uniform (in Fig 10 (a)), which was resulted from the low viscosity of the solution, the low polymer concentration during the electrospinning process as well as the insufficient entanglement degree. Additionally, the electrospinning technology relies on the tension effect from the electrostatic repulsion in the polymer solution, thus small polymer jets will be generated and then solidify into fibers. Consequently, the fiber diameter will obviously increase with the increasing PU concentration, as shown in Fig 10, the fiber uniformity of PU-11, PU-12, PU-13 were improved, because the solution concentration and viscosity increased, thus the solvent would fully volatilize. Likewise, adhesions appeared among PU-14 that was also because the nonvolatile solvent DMF did not completely volatilize, however, it exhibited favorable solubleness for carbamate and polyether in the polyurethane structure. So as to compare with the nanoweb in the following, PU-12 with fiber diameter ranging from 600nm to 700nm were adopted as the optimal samples.

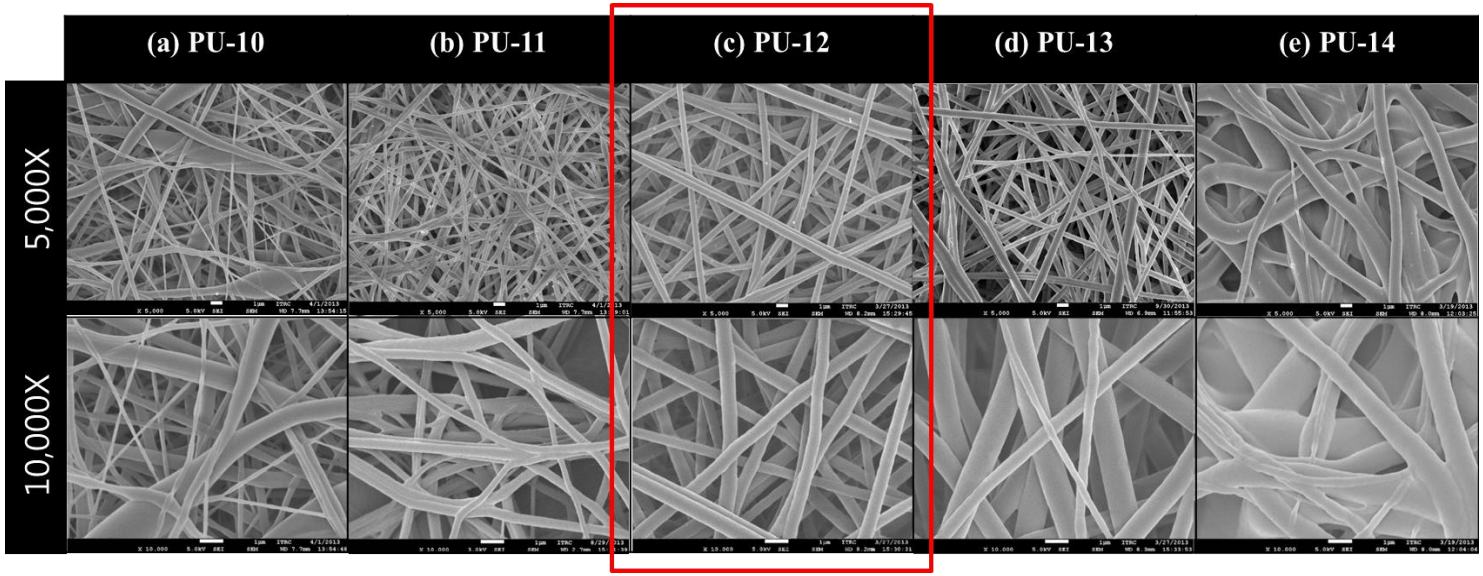

Fig.10. Variation in the morphology of pure PU in DMF/THF electrospun under different processing conditions; (a) 10 wt.% PU, (b) 11 wt.% PU, (c) 12 wt.% PU, (d) 13 wt.% PU, and (e) 14 wt.% PU.

.

1.2 Concentration of PU in the PU/SNPs solution

As is known to all, the surface roughness of the membrane surface is a factor that affects its surface wettability [46]. Therefore, in order to compare pure PU nanoweb with SNPs fiber membranes, we should unify the diameters of their principal fibers (eliminate the increased value caused by the addition of SNPs). The properties of the polyurethane solution would be changed with the increment of SNPs, namely, the more you add, and the higher the solution viscosity will be. Consequently, its conductivity would decrease though the differences for the surface tension of the solution remain limited. Meanwhile, the electrospun nanofibers possesses great differences in its morphology and surface structure when compared with general fibers and the evaporation speed of the solution (DMF/THF) would also be affected as the organics increase. Right before the addition of SNPs, we should thus identify the concentration of PU. As is shown in relevant literature, with the premises of preserving the original property of PU, the maximum addition of SNPs is 10wt%. in this case, as we changes the concentration of PU when preparing for spinning, the concentration of 4wt% SNP and TEOS/acetic acid should not be altered so as to gain the best concentration of PU. Figure11 is the SEM image that suggests the nanoweb membrane produced under the spinning of different PU and 4wt% SNP concentration and a certain value of TEOS/acetic acid density.

In order to get closer to the sizes of the PU fiber diameters so as to prepare for later tests on surface wettability, we compared three PU concentrations which is closest to 600-800nm after multiple tests. As is shown in the Fig 11, typical fiber morphology would still be formed with the addition of SNPs even under low PU concentrations. Besides, with the increases in PU concentrations, the diameters of

the fibers also increase with 748nm, 762nm, 765nm and 827nm relatively for $PU_{7.4}$-SNP_4, $PU_{7.8}$-SNP_4, $PU_{8.2}$-SNP_4 and $PU_{8.6}$-SNP_4. As is suggested in Fig 11, this phenomenon was caused by the increases in solution viscosity and the decreases in conductivity. In addition, the papillae was formed on the fiber surface with a size of 20-50nm. Under the optimum condition of $PU_{8.2}$-SNP_4, the distribution of SNPs is relatively homogeneous without any agglomeration. As for the reasons, it might because of the SNPs' evenly filling into the molecule segments of the PU matrixes and the formation of certain crosslinking in the forms of chemical bonds. Moreover, the added TEOS would turn to be active SNPs with –OH on its surface via the process of hydrolytic condensation in the internal phase. Utilizing the –OH bearing SNPs and the PU covered SiO_2 microsphere elastomers, the inorganic conglomerated particles could well disperse into the organics with the addition of SNPs with sizes of 16-20nm and the PU's separately dispersing in two phases of the emulsion. Meanwhile, the –OH on the surface of SNPs would also react with the –NCO of PU and eventually get bond in the forms of chemical bonds.

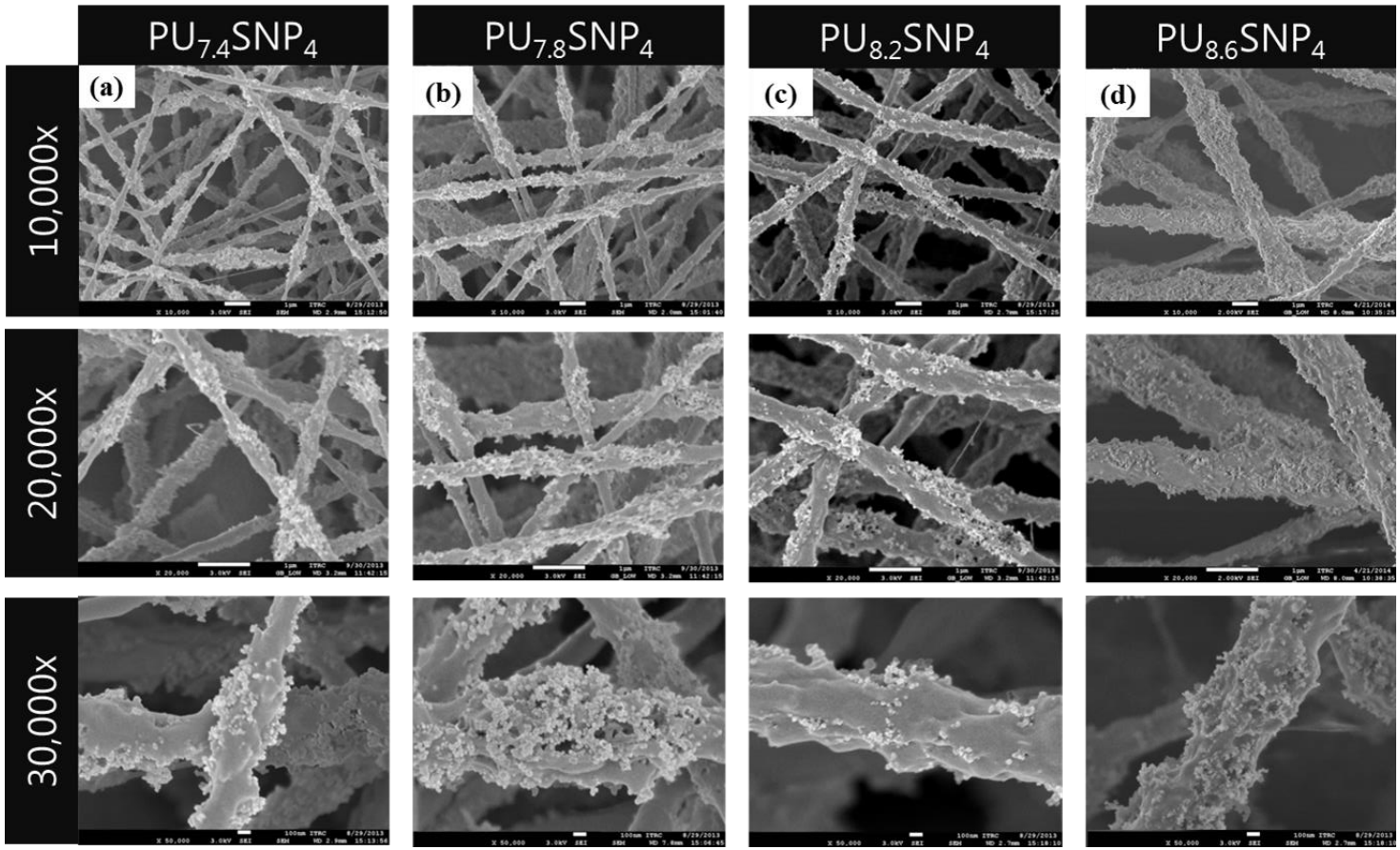

Fig. 11 The Morphology of different concentration of PU solution with the same SNPs webs by electrospinning.

Besides, we also compared the surface morphology of specimen under the condition of no TEOS/acetic acid. As is showed in Fig 12(d), there appears obvious agglomeration of SNPs, namely, the two constituents cannot disperse evenly. Therefore, with the effects and transmission of out-field forces, the SiO_2 particles in the PU/ SNPs hybrid materials in dispersed phases should serve as the focal point of stress. Since cracks would be generated under drawing and compressing forces or the destructive effects of impact and shear due to de bond and cavity, we could only gain best-strength nanoweb membranes with effectively dispersed SNPs.

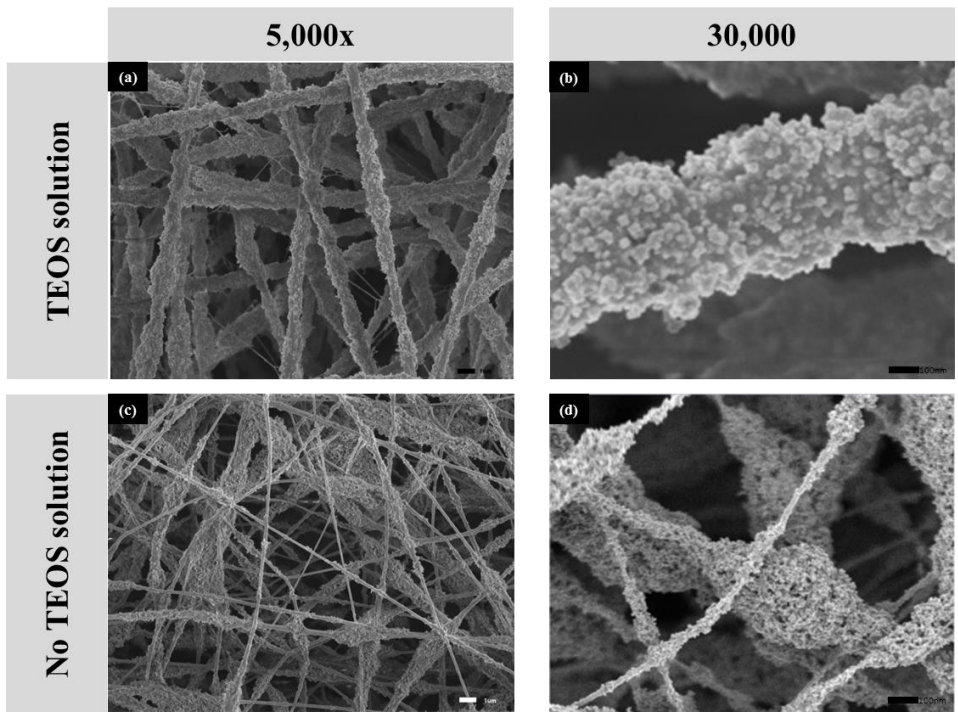

Figure12 Morphology of PU/SNPs nanoweb with and without TEOS/acetic acid solution.

1.3 The structure of PU/SNPs nanofibers with TEOS/acetic acid solution

The microcosmic structure image of PU/SNPs after adding TEOS and SNPs were shown in Fig 13. From the figure, we can find that the silica nanoparticles were rounded bodies with diameters of around 20nm and they are well-distributed relatively without large agglomeration. Fig 11 shows that SNPs were well dispersed in the PU. This shows that when adding a certain amount of inorganics SiO_2 into the organic materials, we can get PU elastomer (shown in Fig 13) modified by silica nanoparticles. The SNPs were grafted the organic materials by sol-gel method, thus enhancing the superhydrophobicity. However, when the SNPs were used in excess of a stipulated rate of mass, the material regularity would be heavily discounted, which reduce the performance of the materials.

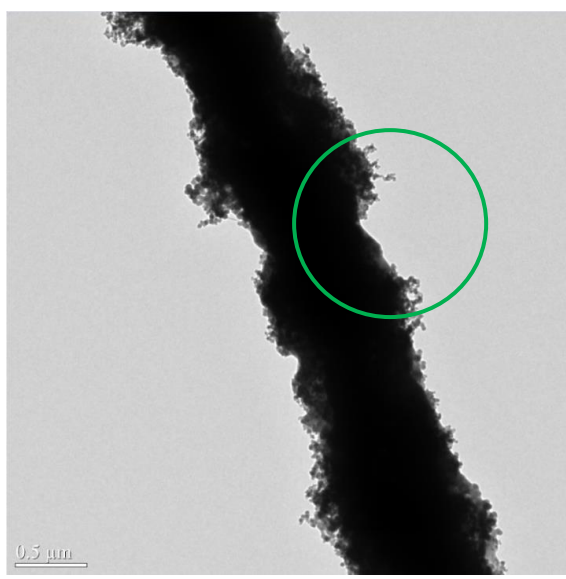

Figure 13. The EF-TEM image of PU/SNPs nanoweb with TEOS/acetic acid solution.

1.4 PU-SNPs nanoweb

Given that the spinning solution would be too ropy to produce good spinnability as the concentration of SNPs reaches 6wt%, the appropriate concentration should be set at 1-6wt%.

The SNPs contents can be varied in a wide range up to 1-6 wt. % (relative to the PU) with good dispersion. The FE-SEM images of electrospun fibrous nanoweb obtained by varying the concentration of PU-SNPs solution are shown in Figure 14. Combined with TEOS/Acetic acid and SNPs. By increasing the SNPs contents, PU-SNP_2, PU-SNP_3, PU-SNP_4, PU-SNP_5, and PU-SNP_6 nanoweb exhibited increased fiber diameters, which were related to the enhanced viscosity and conductivity of the composite solution.

Silica nanoparticles would spread on the PU-SNPs fiber surface prepared, and the presence of these particles greatly increases the surface roughness of the fiber surface, and the hydrophobicity of the fiber membranes will also be improved, especially the PU-SNP_5 fiber membrane. As DMF turns to be the most abundant material in the compounded solvent (As the content of DMF in the compounded solvent surpasses that of any other materials), the solvent volatilization rate continues to slow. . However, it would lead to incomplete volatilization of the solvent inside fibers, extremely slow forming of nanoweb, and agglomerations among fibers when only DMF is added. Therefore, the relatively high-speed volatilization of THF was added and the inside solvent can properly volatilize during the spinning process of PU-SNP_s solution when volume ratio of DMF/THF is 4:1[37]. After adding silica nanoparticles, the particles had enough time and opportunity to reach the fiber surface along with the solvent, and therefore quite many silica nanoparticles appeared on the fiber surface. The particles added may

change the nature of the solution, but also hindered the phase separation of the jet flow, so excess SNPs would lead to a decline of roughness of the fiber surface.

Moreover, gradually increased nano-protrusions in the range of 20–50nm were clearly visible on the fiber surface as SNPs contents were increased, which formed nano-micro structures roughness (protrusions/nanoweb). The PU-SNP_5 and PU-SNP_6 nanoweb showed good distribution of protuberances on the surface of the fibers without aggregation. This could be ascribed to the fast evaporation of the solvent during electrospinning, thus leading to the phase separation before the polymer solidification and the existence of the interaction between PU and SNPs, meanwhile, TEOS also played an assisting role between PU and SNPs. But the average of PU-SNP_6 fiber diameter was larger than PU fibers (fiber diameter: 1000nm~1300nm). In relatively humid environment, the conductivity of acetic acid will increase during spinning, so there will be a small amount of spider-fibers generated during the spinning process[71].

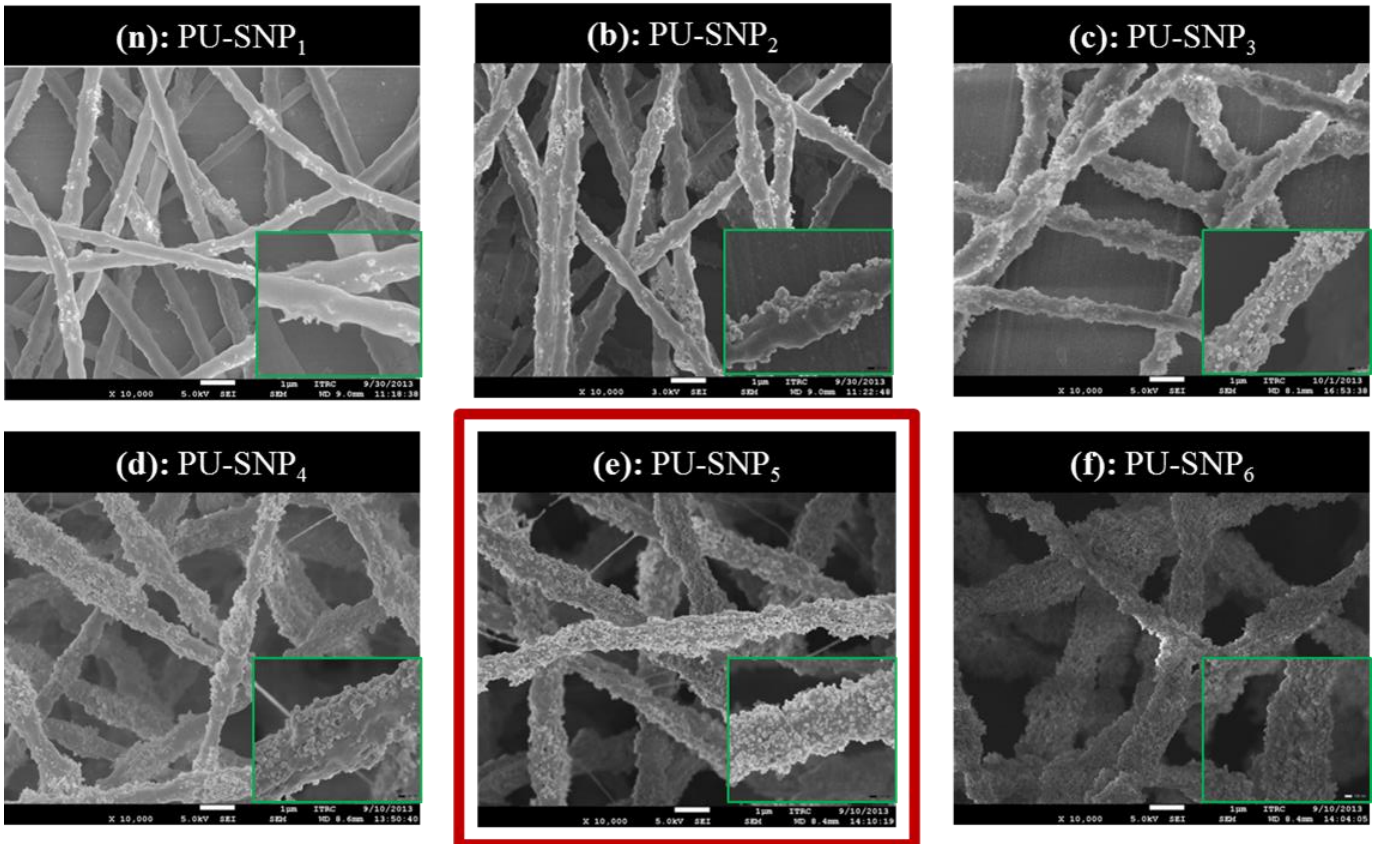

Fig. 14. The Morphology of different concentration of PU solution with the same SNPs nanoweb by electrospinning.

1.5 PU-SNPs-CVD nanoweb

The PU web and PU-SNPs nanoweb were had the hydrophobicity by DTMS CVD at 150 ℃ for 3h in vacuum oven. The morphology of the CVD treatment nanoweb was not significantly changed as shown in Fig 15.

Uniform fibers were obtained from PU nanoweb, PU-CVD nanoweb, PU-SNPs nanoweb and PU-SNPs-CVD nanoweb. The mean fiber diameters of PU nanoweb, PU-CVD nanoweb, PU-SNPs nanoweb and PU-SNPs-CVD nanoweb were measured as 648, 678, 752 and 729 nm.

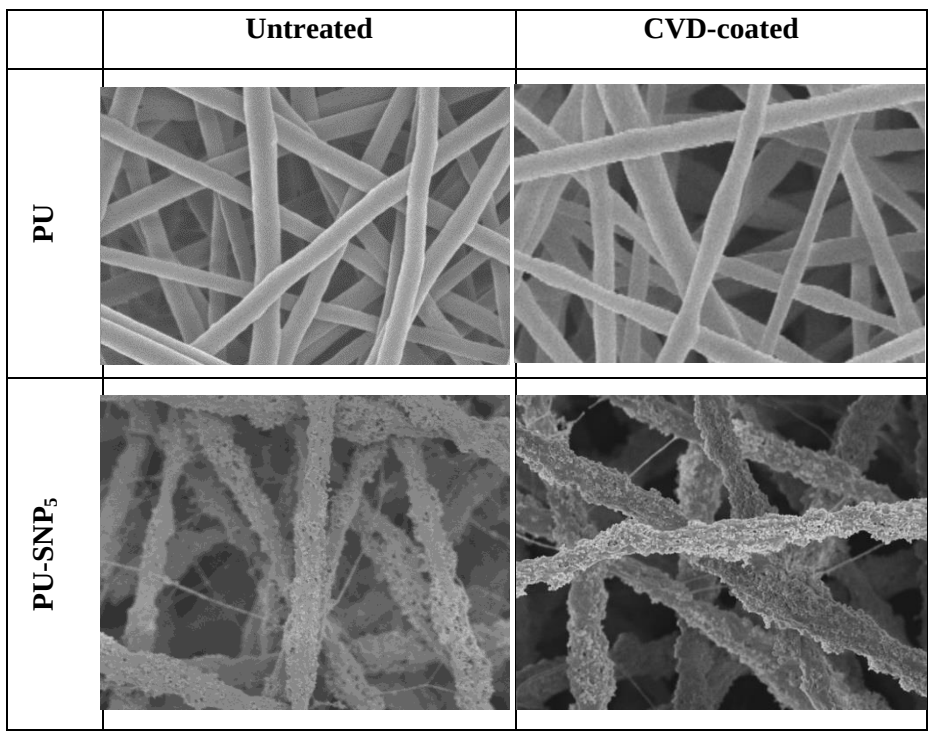

Figure15. FE-SEM image of PU nanoweb and PU/SNP_5 nanoweb with and without DTMS treatment.

2. Mechanical property

Mechanical behavior data of the PU/SNPs nanoweb, which were converted from measured loads versus cross-head displacements, are presented in Figure16 (1)-(2).

The different mass fraction of PU-SNPs nanoweb was prepared to observe an influence of the mechanical property by electrospinning. The smaller the chain extension coefficient was, the bigger the cross-linking density would be. Testing result of tensile splitting strength of the PU/SiO_2 composite nanoweb prepared according to different chain extension coefficients can be seen in Fig 16. As indicated in Fig 16, both the tensile strength and the break of the PU/SiO_2 composite nanoweb had been decreased when compared with PU nanoweb. The tensile strength first rose and then fell, with the overall elongation being increased dramatically, and the comprehensive property was at its best when the force was increased by 3wt%. The mechanical strength of the PU nanoweb increased along with the increasing of the chain extension coefficient. The hardness of the PU/SiO_2 composite material was slightly improved than that of the PU, which could be taken as that the composite materials had higher hard-segment contents. When there were higher hard-segment contents, the micro-phase separation would be larger and the mechanical property would be better.

When the PU nanoweb were used in solid state, the mechanical strength embodied under various external forces was the most important indicator of its usability[72, 73]. There were several reasons for adding SiO_2 to improve mechanical strength: (1) when the material was under external forces, SiO_2 particles could bear certain load and thus consumed part of the accumulated energy generated by stress; besides, these inorganic particles diverged or changed the

directions of cracks, which dispersed the stress, stopped the further development of cracks, delayed the break, and improved the mechanical property of the materials. (2) SiO_2 not only scattered in the PU groups increasing the randomness of soft and hard chain segments, it also led to heterogeneous nucleation and improved the mechanical strength of the PU material, for the chemical bonds or the hydrogen bonds formed by hydroxyl on the surface of the SiO_2 particles and the isocyanate group in the PU macromolecule was helpful for the crystallization of the macromolecule. Therefore, adding SiO_2 improves the concentration of the hard chain segments in composite materials. The improvement of the concentration of the hard chain segments helped to improve mechanical property. With the increasing of PU hard chain segment contents, the tensile strength increased and the elongation fell. The elongation at break of the PU/SiO_2 composite material was higher than that of PU, and as indicated by data in the figure: the decrease magnitude of the elongation reached the least level when SNPs was added by 3wt%.

When the SNPs content was 5wt%, tensile strength at break was not significant decreased to observe in the various PU-SNPs nanoweb, and observing the previous SEM (in Figure17), the nanoparticles were distributed evenly and widely on the nanofibers surface , as a result the improvement of surface roughness by SNPs had an influence on Superhydrophobicity. According to the above analysis, 5wt% PU-SNPs nanoweb was the best choice for later assessment. Analysis of shapes and appearances for the tensile fracture surface of PU/SNPs composite materials were shown in Fig 16.

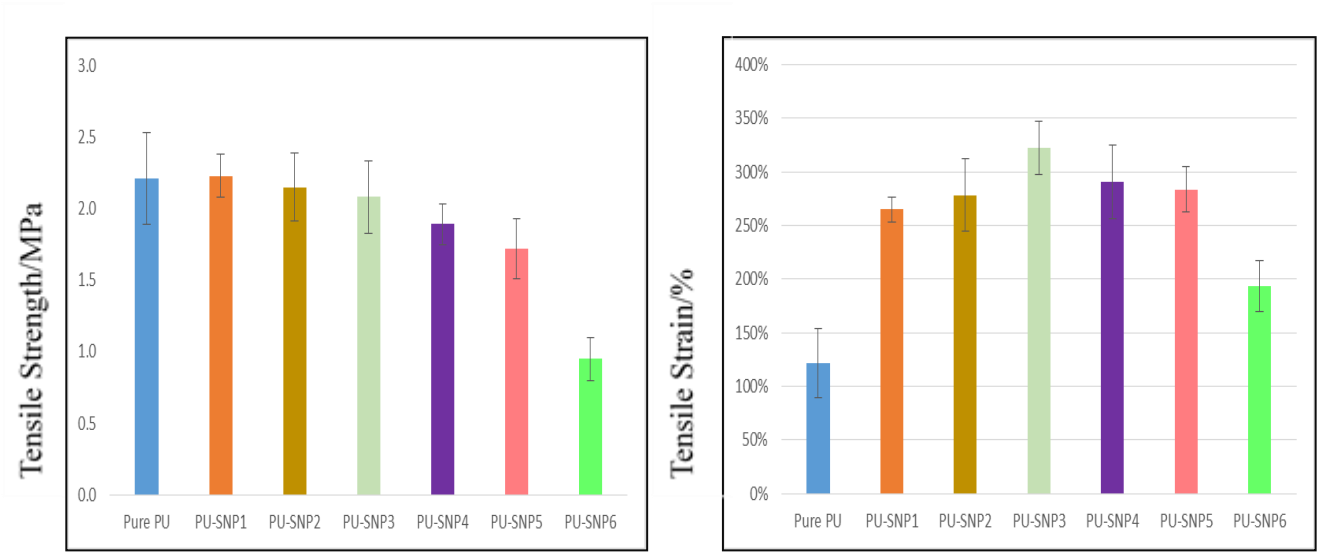

Fig 16. Tensile strength of the electrospun PU/SNPs nanoweb with different mass rate of SNPs.

According to the strain-stress behavior, it could be seen that composites with 5wt % SNPs content possessed preferred mechanical properties. To further understand the relationship among SNPs contents, and mechanical properties, the dispersion of SNPs in PU was analyzed by SEM. As shown in Fig 17 slight agglomerations of SNPs are observed in PU matrix (Fig 17). However, all the SNPs were dispersed well in PU matrix (Fig 17). It was believed that with addition the TEOS, the SNPs surface were grafted with a large number of active groups and the concentration of oxygen functional groups on its surface were greatly improved and so the interface property was improved substantially. Therefore, PU-SNP_5 nanoweb were chosen as an optimal PU solution concentration for PU-SNPs nanoweb (fiber diameter: 600-800nm).

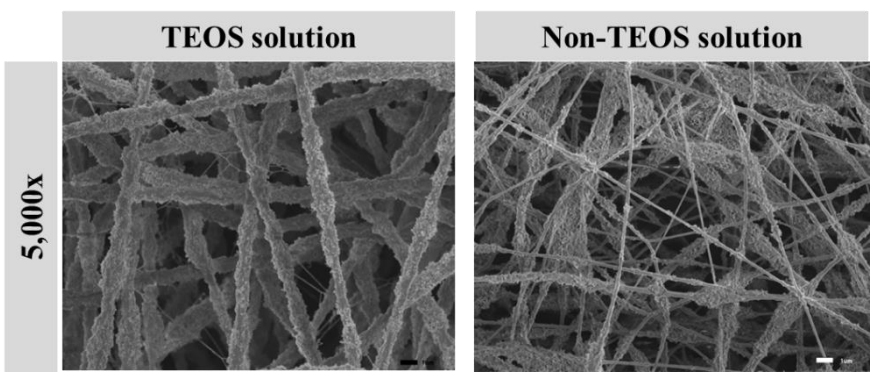

Figure 17. Morphology of PU/SNPs nanoweb with and without TEOS/acetic acid solution.

3. Surface chemical property

From Figure 18, an FTIR spectra of PU polymer, we can notice high frequency absorbing peaks, appeared in the 1,700-1,670 cm^{-1} region, owing to stretching vibration of C=O bond in carbamate (R— O—C(=O)—NHR). In general, high frequency absorbing peaks corresponding to amino-substituent and to a dis-substituted compound might occur in the region of 1,736–1,700 cm^{-1}. A combination of the both gave rise to the peak of 1,730 cm^{-1}. Attributed to C=O stretch of amide-group there was also 1,701 cm^{-1} region. The characteristic bands of alkyl ether produced the wide 1,106 cm^{-1} (1,150-1,060 cm^{-1}) and 1,079 cm^{-1} regions because of the C—O—C cm^{-1} asymmetrical flexing vibration. The a like regions in Figure12 indicated the existence of PU polymer in the composite fibers according to the appearance of 2,939, 2,859, 1,730, 1,702, 1,479, 1,109, and 1,080 cm^{-1} region. Because of the configuration of SiO_2 crystal, there appeared 1,059-1,067 cm^{-1} bond associated with the stretching and angular vibrations of the skeletal Si—O—Si bond, which is an Eigen vibration range of the peak value. Thus, multiple absorbing peaks of 649 cm^{-1} and 609 cm^{-1} were shifted from 664 $cm^{-1}$and 611 cm^{-1} of PU polymer (PU web). Moreover, compared with PU membrane, the intensity of the FTIR in electrospun PU/SiO_2 fibers in 3,405, 2,272, and 1730 cm^{-1} region decreased.

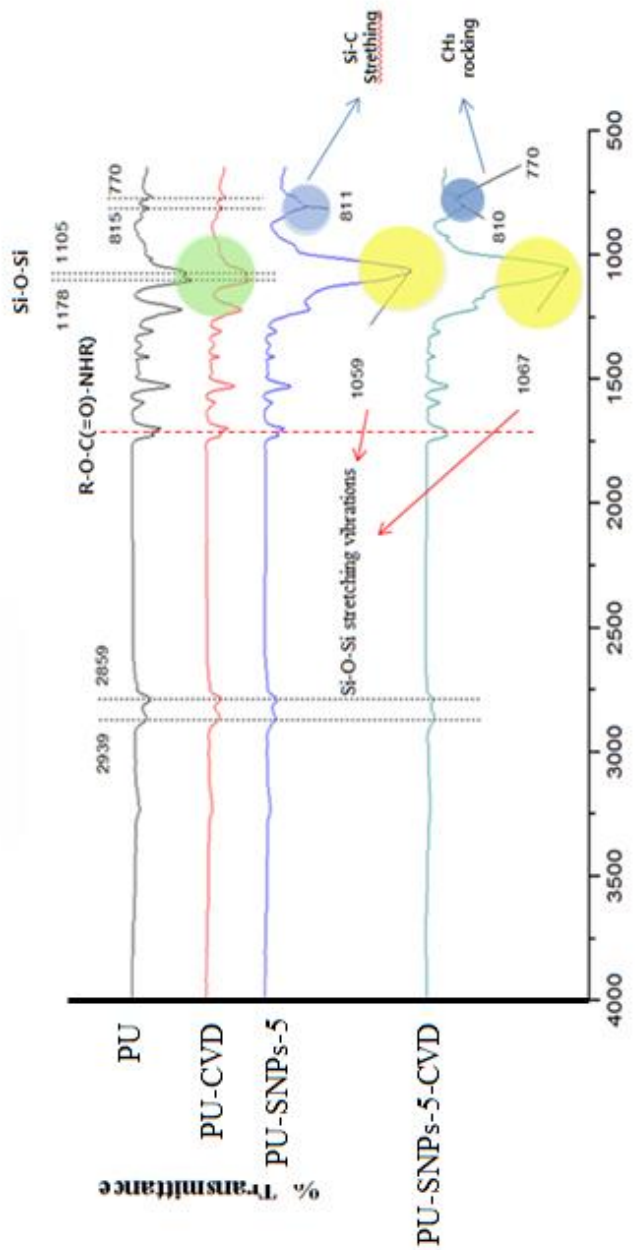

Figure 18. FTIR image of PU, PU-CVD, PU-SNP_5 and P-SNP_5-CVD nanowebs.

For the surface of CVD-P-T-SNPs nanoweb, Si-C and –CH, -CH_3 peaks appear at wave numbers of 1059, 811cm^{-1} which was corresponding to Si-O-Si stretch vibration , Si-C stretching vibrations and –CH_3 as well as –CH_2 stretching vibrations respectively, whereas such peaks are absent in the SNPs. But PU-CVD nanoweb did not significant showed and Si-C stretching vibrations and –CH_3 stretching vibrations.

Chemical composition of the PU-SNP_5 nanoweb was verified by energy dispersive X-ray (EDX) spectroscopy. Figure 19 displays EDX micrographs of an unmodified PU nanoweb, PU-SNPs, PU-CVD and PU-SNP_5-CVD nanoweb. The PU nanoweb do not contain any contaminants, indicated by the sole presence of carbon (C), nitrogen (N) and oxygen (O) atoms. , PU-SNP_5, PU-CVD and PU-SNP_5-CVD nanoweb reveals that the SNPs modified PU nanoweb contains only silicon (Si), carbon, nitrogen and oxygen atoms, indicating high purity of SNPs

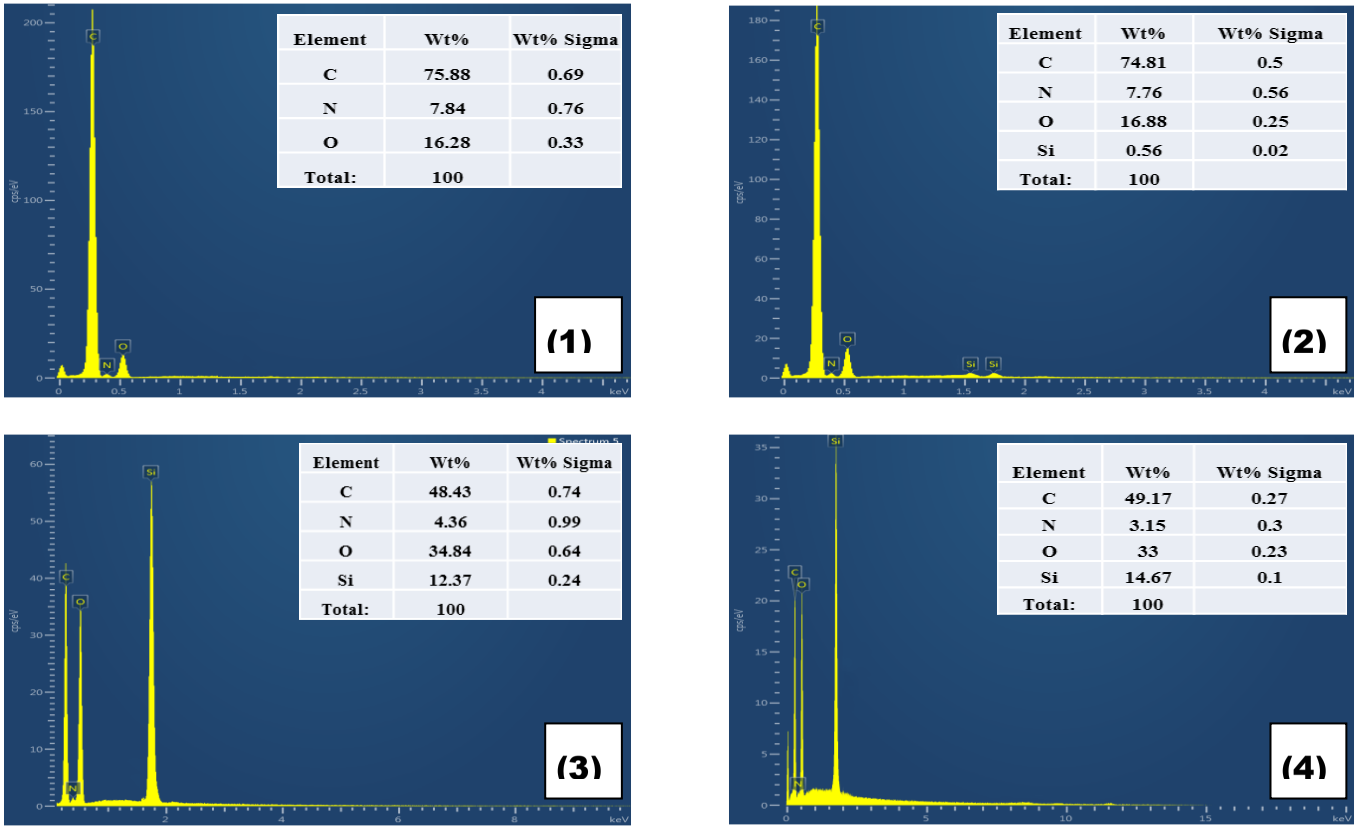

Fig. 19. EDX spectra of the PU nanowebs (1), PU-CVD nanowebs (2), the PU-SNP_5 nanowebs (3), PU-SNP_5-CVD nanowebs (4).

4. Surface wettability

4.1 Static contact angle

The polyurethane is a thermoplastic elastomer composed of hard segments (diisocyanate) and soft segments (polyether). The carbonate groups in hard segments and the ether groups in soft segments provide comparable hydrophilicity, thus leading to high surface energy which is larger than 40 mN m^{-1}[47]. On the other hand, the PU casting film has shown hydrophobicity with WCA of 93° by aluminum substructure. Figure20 shows that the WCA of PU nanoweb, PU-CVD nanoweb, PU nanoweb and PU-SNP_5-CVD nanoweb increased from 131° to 159°. As shown Figure 21, it could be attributed to the increased size of the fiber diameter leading to increased roughness of the nanoweb. A rough surface could trap more air under the water droplet. Because of DTMS treatment lower surface energy of PU-SNP_5-CVD, WCA was slightly increased on nanoweb surface.

Previous experiments are not conclusive regarding the optimization of distribution of bumps present on the surface. The relationship of air pocket formation and geometric parameters needs to be shown. This information is critical in designing a superhydrophobic surface for applications which require water repellency[74]. In this study, Experiments are also conducted to the contact area of water droplet and nanoweb is decreased and the superhydrophob ic property of PU/SNPs nanowebs membrane is improved significantly.

This reduces the area that fiber surface can contact the droplets, thereby greatly improves the superhydrophobic properties of pure PU / SNPs fiber membrane.

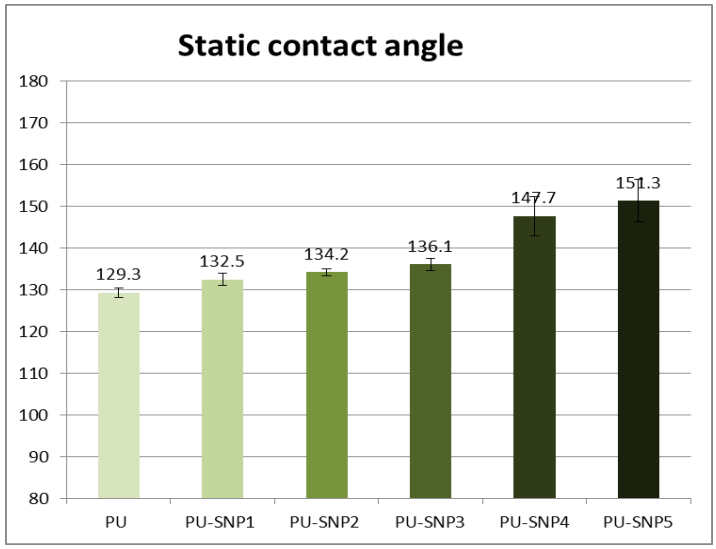

Figure20. Static contact angle of the electrospun PU/SNPs nanoweb with different mass rate of SNPs.

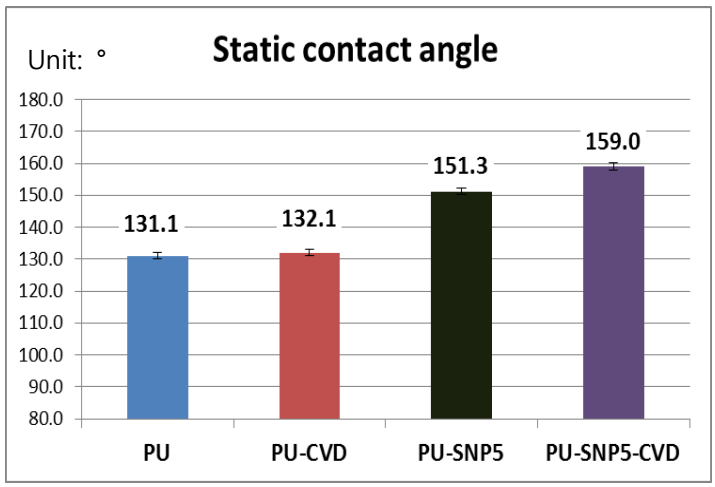

Figure 21. Static contact angle of the different nanoweb with and without DTMS treatment.

4.2 Shedding angle

As hydrophobicity is related to static contact angle and dynamic contact angle, WSA with super hydrophobic surface can describe the liquid-solid interface free energy, so we carried out investigation on the shedding angle of PU nanoweb. Results showed that when we dropped 12.5μL liquid on the PU-SNPs nanoweb whose static contact angle (WCA) was as large as 151.3°, the liquid drops always adhered to the surface of the web, as shown in Fig 22-23. Shedding angle PU-SNP_5 was 32.6°. The surface of PU-SNPs membrane had a very high WCA. However, the shedding angle of PU-SNP_5-CVD was only 5°. Even if the surface of membrane had a multi-scale roughness, no roll-off phenomenon would appear. That's because the surface energy of polyurethane is relatively larger; so even if a contact angle of 150° was obtained, the shedding angle would still be very large. Therefore, it should be attributed to the combination of multi-scale roughness of nanweb and low surface energy by DTMS that the shedding angles on the surface of membrane were significantly different.

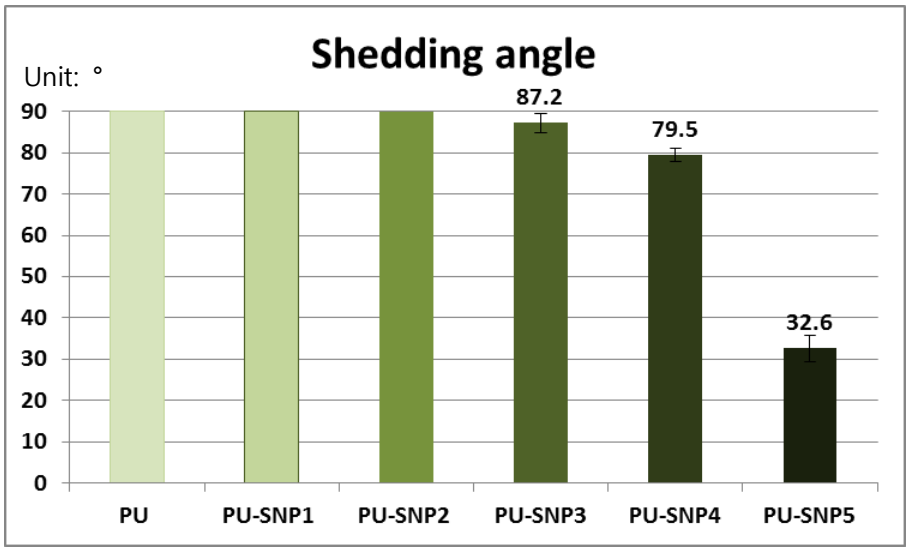

Figure22. Shedding angle of the electrospun PU/SNPs nanoweb with different mass rate of SNPs.

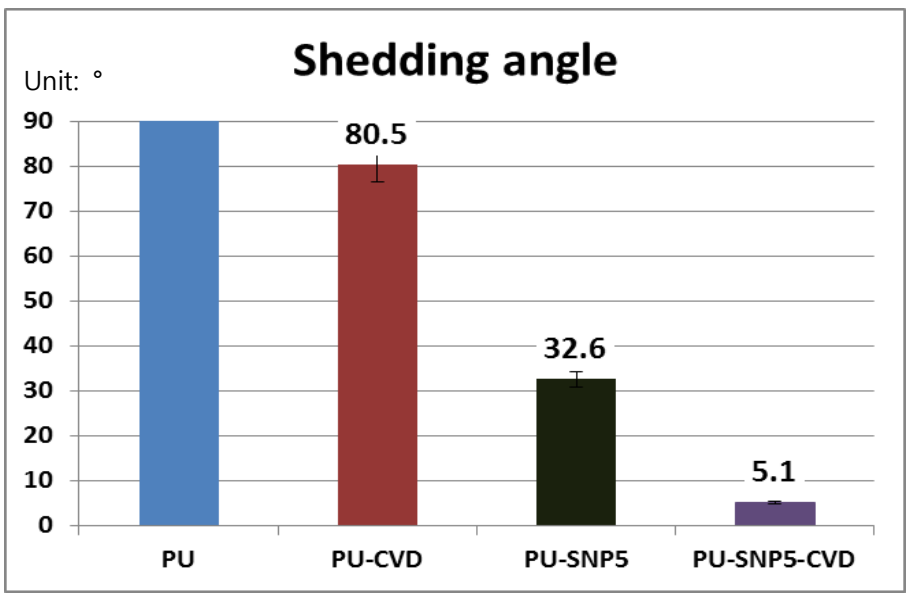

Figure23. Shedding angle of the different nanoweb with and without DTMS treatment.

5. Transport property

5.1 Air permeability

We measured the porous structure air permeability of nanoweb through the air gas adsorption test and investigated the influence of the roughness that resulted from SNPs content air permeability of PU, PU-CVD, PU-SNPs and PU-SNP_5-CVD nanoweb were shown in the Fig 24, the flow rates of PU web, PU-SNP_5, PU-SNP_5-CVD were showed good air permeability under low pressure (below 50 PSI), which exceed 200 cc/sec[75], but the flow rate of pure PU-SNP_5 was relatively higher than that of the other three nanoweb.

Xue et al. report [76], when the solution viscosity decreases, fiber diameter will decrease, the arrangement between fibers will become closely, resulting in a decrease in the fiber pore size and the air permeability of nanoweb. When solution concentration increases, fiber diameter will increase, the arrangement between fibers will become loose, forming more air gaps, the air permeability will significantly increase. During composite spinning by adding SNPs with different mass concentration, membrane with relatively thick nanofibers will be formed, preventing the close arrangement between fine fibers, increasing the distance between the nanofibers, therefore, its air permeability is improved compared to the fiber membranes made in pure PU solution. During the CVD processing phrase, a small quantity of water molecules will be generated when heated with high temperature, as a result, SiO_2 particles will be formed by sol-gel method when DTMS reacts with water, the transmission of water vapor will be influenced as well [77].

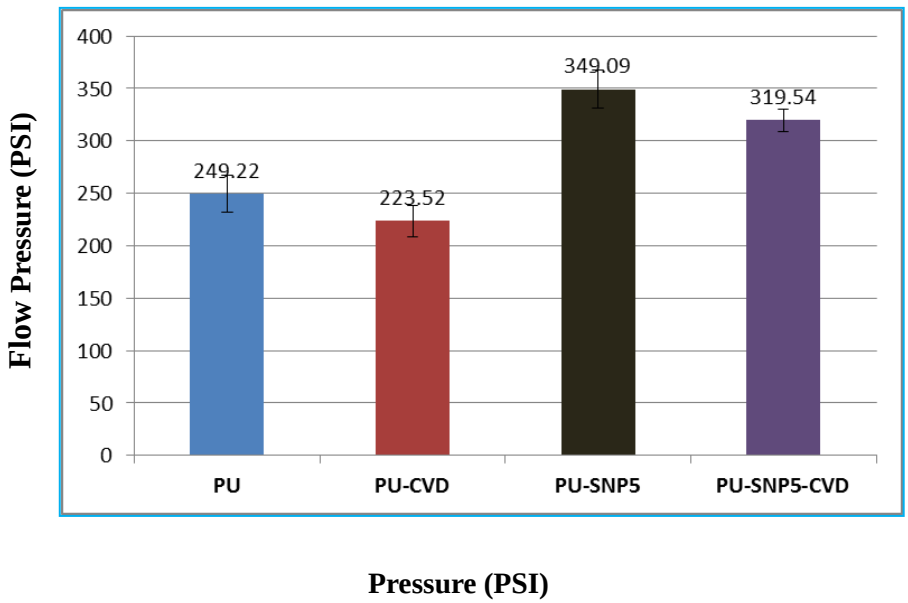

Figure 24. Air permeability of the different nanoweb with and without DTMS treatment.

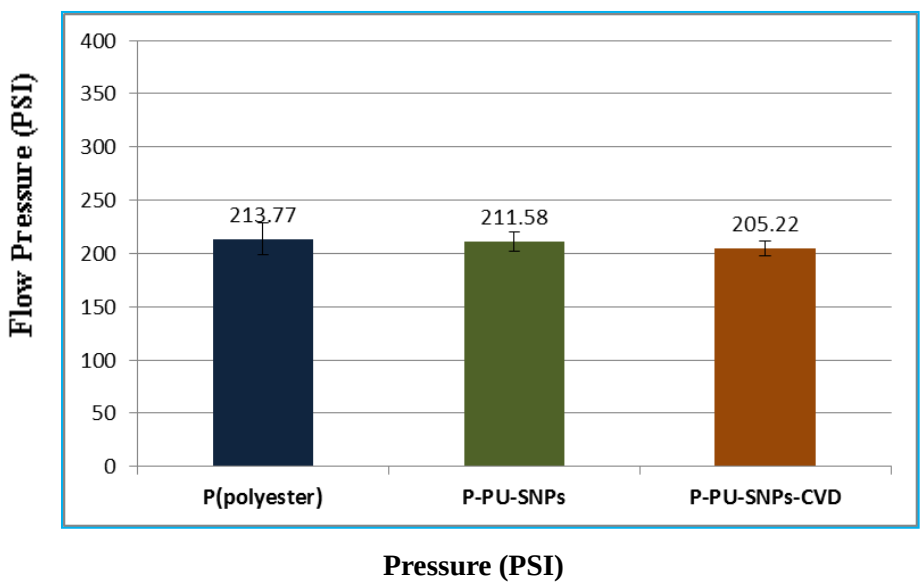

Figure 25. Air permeability of polyester fabric, nanoweb laminate polyester and nanoweb laminate polyester with DTMS treatment.

5.2 Water vapor transmission

Water vapor transmission of nanoweb is the important factor which influences on clothing comfort of the wearer. Perspirations can be transferred through a textile material in the form of water vapors in normal conditions and water liquids in special conditions such as during hard exercise. The nanoweb itself has good pore dispersion rate and micron- even nano-scale thickness so that it has very strong water vapor transmission. However, studies conducted on nanoweb which are processed and produced directly as fabrics are still premature. In most circumstances, nanoweb is put into production as laminate. Based on the research, it was found that PU-SNP_5-CVD nanoweb contained superior superhydrophobicity and breathability. Therefore, the electrospinning nanoweb and nanowebs laminate polyester fabrics were prepared to observe in this research. The electrospinning parameters of PU-SNP_5-CVD nanoweb laminate polyester remained same.

In this research, Water vapor transmission was measure by "calcium chloride method" according to ASTM E 96: KS K0594. Because of a gradient of relative humidity between inside and outside of a cup, water vapor was transferred through a textile. That is, water vapor passed out from the environment inside of cup. Water vapor was absorbed by desiccant. The quantity of absorbed vapor was defined by weighting and water vapor transmission (WVT) was calculated.

Figure 26 showed the WVTR of PU, PU-CVD, PU-SNP_5 and PU-SNP_5-CVD. The entire nanoweb showed great WVTRs which exceed 5000 $g/m^2/h$, because of porous architecture of electrospun nanoweb. PU showed the greatest WVTR of 7362 $g/m^2/h$, but after CVD coating WVTR slightly decreased to 7263 $g/ m^2/h$. It is speculated that after CVD process, As the surface has been hydrophobic treated,

then the surface energy of PU-SNP_5-CVD has been significantly reduced, leading to a decline in moisture permeability of PU-CVD, PU-SNP_5-CVD nanoweb that have been processed by CVD [77]. On the other hand, DTMS molecules blocked some pores by hydrophobic treatment [31]. PU nanoweb showed smaller WVTR than PU-SNP_5 nanoweb because PU-SNPs solution concentration increases, fiber diameter will increase, the arrangement between fibers will become loose in electrospun nanoweb, and PU-SNP_5 had better WVTR than PU-CVD because SNPs blocked pores in electrospun nanoweb. It also support that lower surface energy had an effect on WVTR. For these reasons, PU-SNP_5-CVD had smallest WVTR.

Based on theoretical analysis, the factors influencing water vapor transmission include the fabrics' pore size, the number of pores, and the fabrics' thickness. Under the normal state of the water vapor diffusion, it was found that the bigger the pore size was, the greater the water vapor diffusion was in the free cross-sectional area. Accordingly, the wet resistance was also smaller, which caused greater water vapor transmission. The image Fig 27 showed the WVTR of polyester fabrics, P-PU-SNPs nanoweb laminate and P-PU-SNPs-CVD nanoweb laminate, the results measured according to ASTM E 96: KS K0594 standards of the fabrics are respectively 6211.0, 6161.6, 6082.3g/m^2•24h presenting a downward trends.

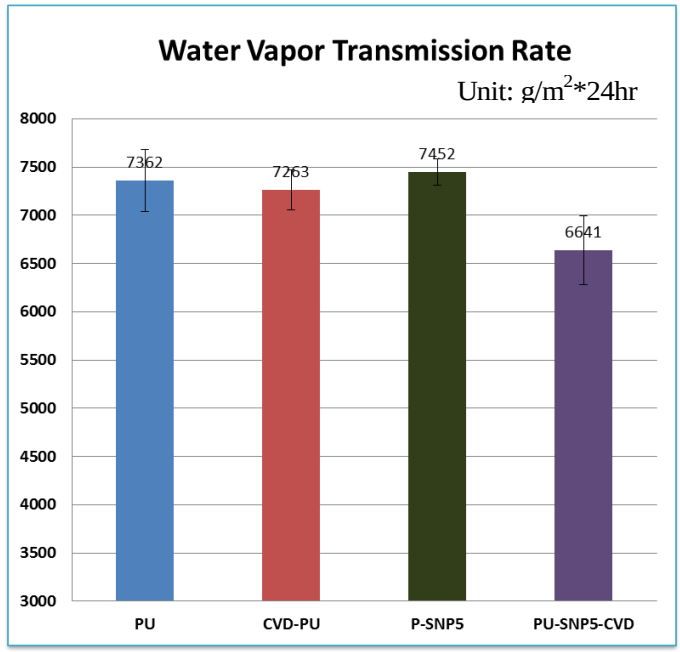

Figure 26. The WVTR of PU nanoweb, PU-CVD nanoweb, PU-SNPs nanoweb and PU-SNP_5-CVD nanoweb.

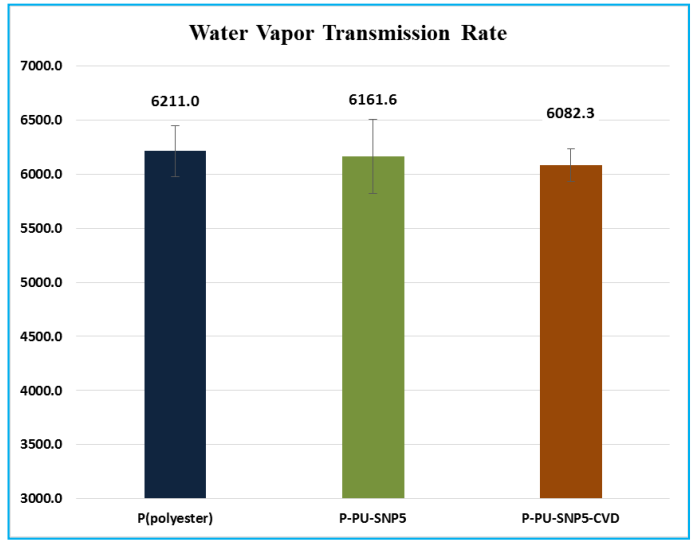

Figure 27. The WVTR of polyester fabrics, P-PU-SNPs nanoweb laminate and P-PU-SNPs-CVD nanowebs laminate.

According to the test result of the air permeability and water vapor transmission in the PU-SNP_5 nanoweb and PU-SNP_5-CVD nanoweb, it was found that the air permeability and light transmission of fiber membrane fell relatively with the hydrophobic treatment. In the same way, the pristine Polyester, Polyester--PU-SNP_5, Polyester-PU-SNP_5-CVD also presented a downward trend.

Seoug et al. [78] reported that clothing with higher than 5000 $g/m^2/h$ of WVTRs passes water vapor sufficiently so that the wearer feels comfortable with the clothing. However, in any circumstance, the water vapor transmission of the Polyester-PU-SNP_5 laminate which had gone through the electrospinning, had reached the general standard of the PTFE laminate fabric clothing [79]. From that, we could see the microporous PolyesterPU-SNP_5 laminate which had gone through the electrospinning had excellent water vapor transmission, superhydrophobicity and breathability.

IV. Conclusion

This research was aimed to obtain breathable superhydrophobic nanowebs, using polyurethane and SiO_2 nanoparticles by electrospinning and chemical vapor deposition. Water contact angle and shedding angle were measured to identify the Superhydrophobicity of surfaces. Tensile stress-strain, water vapor and air permeability were also evaluated. Results are as follows:

1. By observing appearance of fibers, SNPs was seen to be able to distribute evenly on the surface of nanowebs surface when TEOE/acetic acid solution had been added.

2. Tensile strain of PU was found to be improved by adding SNPs and the tensile strength was reduced within the range of 1wt%-5wt%.

3. Maximum contact angle of 159° and minimum shedding angle of 5° were obtained at the condition of 5wt% SNP concentration and DTMS chemical vapor deposition at 150℃ for 3h.

8. The addition of SNPs enlarged gaps among fibers, and thus PU-SNP_5 nanowebs possessed a better breathability than PU nanowebs. Besides, a 200cc/min (below 50 PSI) still remained when it was made into nanowebs laminate.

9. Gaps among fibers were enlarged due to addition of SNPs. Therefore, water vapor transmission rate of PU-SNP_5 nanowebs was better than that of PU nanowebs. However, water vapor transmission rate was reduced after the hydrophobic process, though a high pass-ability still remained (6641g/m^2*24h). In addition, it reached 6082g/m^2*24h after being made into nanowebs laminate. As shown by the above results, PU/SNPs nanowebs had better

Superhydrophobicity and breathability when compared with PU nanowebs. Besides, there were no significant changes in water vapor transmission permeability and breathability of PU/SNPs nanowebs after it was made into PU/SNPs nanowebs laminate.

V. Reference

1. Bahners, T., *The Do's and Don'ts of Wettability Characterization in Textiles.* Journal of Adhesion Science and Technology, 2011. **25**(16): p. 2005-2021.
2. book, *self-cleaning materials-lotus effect surfaces*. book.
3. Ji, J., J. Fu, and J. Shen, *Fabrication of a Superhydrophobic Surface from the Amplified Exponential Growth of a Multilayer.* Advanced Materials, 2006. **18**(11): p. 1441-1444.
4. Milne, A.J. and A. Amirfazli, *The Cassie equation: how it is meant to be used.* Adv Colloid Interface Sci, 2012. **170**(1-2): p. 48-55.
5. 郭志光, 陈.徐., *仿生超疏水表面的最新应用研究.* 化学进展, 2012.
6. Hashizume, R., et al., *Morphological and mechanical characteristics of the reconstructed rat abdominal wall following use of a wet electrospun biodegradable polyurethane elastomer scaffold.* Biomaterials, 2010. **31**(12): p. 3253-65.
7. •, Y.G.Y.H.S.F. and G.G.F.-L. Qing, *<A Novel Self-Cleaning Coating with Silicon Carbide Nanowires.pdf>.* Mater Science, 2009.
8. Arantes, T.M., et al., *Synthesis and optimization of colloidal silica nanoparticles and their functionalization with methacrylic acid.* Colloids and Surfaces A: Physicochemical and Engineering Aspects, 2012. **415**: p. 209-217.
9. Cai, Y., et al., *Weak acid-base interaction induced assembly for the formation of berry-like polystyrene/SiO2 composite particles.* Materials Chemistry and Physics, 2013. **137**(3): p. 796-801.
10. Crick, C.R. and I.P. Parkin, *Superhydrophobic silica films on glass formed by hydrolysis of an acidic aerosol of tetraethylorthosilicate.* Journal of Materials Chemistry, 2011. **21**(25): p. 9362.
11. Gao, Y., et al., *Novel superhydrophobic and highly oleophobic PFPE-modified silica nanocomposite.* Journal of Materials Science, 2009. **45**(2): p. 460-466.
12. Guo, S.Z., *Preparation and characterization of organic-inorganic hybrid nanomaterials using polyurethane-b-poly[3-(trimethoxysilyl) propyl methacrylate] via RAFT polymerization.* eXPRESS Polymer Letters, 2009. **4**(1): p. 17-25.
13. Kim, H.S., et al., *Urushiol/polyurethane-urea dispersions and their film properties.* Progress in Organic Coatings, 2009. **65**(3): p. 341-347.
14. Ma, J.-Z., J. Hu, and Z.-J. Zhang, *Polyacrylate/silica nanocomposite materials prepared by sol-gel process.* European Polymer Journal,

2007. **43**(10): p. 4169-4177.
15. Raju, K.K.J.a.K.V.S.N., *Synthesis and Characterization of Hyperbranched Polyurethane Hybrids Using Tetraethoxysilane As Cross-Linker.* Ind. Eng. Chem. Res. 2008,, 2008. **47**(23): p. 9214-9224.
16. WERNER STOBER, A.F., *Controlled growth of monodisperse silica spheres in the micron size range.* COLLOID AND INTERFACE SCIENCE, 1968.
17. Xiaojuan, L., et al., *Synthesis and characterizations of waterborne polyurethane modified with 3-aminopropyltriethoxysilane.* Polymer Bulletin, 2010. **65**(1): p. 45-57.
18. Yang, H., et al., *Functional silica film on stainless steel mesh with tunable wettability.* Surface and Coatings Technology, 2011. **205**(23-24): p. 5387-5393.
19. Zhou, H., et al., *The polyurethane/SiO2 nano-hybrid membrane with temperature sensitivity for water vapor permeation.* Journal of Membrane Science, 2008. **318**(1-2): p. 71-78.
20. Niu, J.J. and J.N. Wang, *A Novel Self-Cleaning Coating with Silicon Carbide Nanowires.* The Journal of Physical Chemistry B, 2009. **113**(9): p. 2909-2912.
21. Wang, J., et al., *Synthesis of superamphiphobic breathable membranes utilizing SiO2 nanoparticles decorated fluorinated polyurethane nanofibers.* Nanoscale, 2012. **4**(23): p. 7549-56.
22. Wang, X., et al., *Engineering biomimetic superhydrophobic surfaces of electrospun nanomaterials.* Nano Today, 2011. **6**(5): p. 510-530.
23. Li, C.-Y., et al. *ORMOSILS as matrices in inorganic-organic nanocomposites for various optical applications*. 1992.
24. Sheen, Y.-C., et al., *Non-fluorinated superamphiphobic surfaces through sol-gel processing of methyltriethoxysilane and tetraethoxysilane.* Materials Chemistry and Physics, 2009. **114**(1): p. 63-68.
25. Zhu, J., et al., *Synthesis and characterization of superhydrophobic silica and silica/titania aerogels by sol-gel method at ambient pressure.* Colloids and Surfaces A: Physicochemical and Engineering Aspects, 2009. **342**(1-3): p. 97-101.
26. Acatay, K., et al., *Tunable, superhydrophobically stable polymeric surfaces by electrospinning.* Angew Chem Int Ed Engl, 2004. **43**(39): p. 5210-3.
27. Asmatulu, R., M. Ceylan, and N. Nuraje, *Study of superhydrophobic electrospun nanocomposite fibers for energy systems.* Langmuir, 2011. **27**(2): p. 504-7.
28. Ding, B., et al., *Fabrication of a super-hydrophobic nanofibrous zinc*

oxide film surface by electrospinning. Thin Solid Films, 2008. **516**(9): p. 2495-2501.
29. Ding, B., et al., *Polyamide 6 composite nano-fiber/net functionalized by polyethyleneimine on quartz crystal microbalance for highly sensitive formaldehyde sensors.* Journal of Materials Chemistry, 2011. **21**(34): p. 12784.
30. Jun Zeng, A.A., ‡ Frank Czubayko,‡ Thomas Kissel,§ Joachim H. Wendorff,† and and A. Greiner, *Poly(vinyl alcohol) Nanofibers by Electrospinning as a Protein delivery system and the retardation of enzyme Release by Additional Polymer Coatings.* Biomacromolecules, 2005.
31. Kang, M., et al., *Preparation of superhydrophobic polystyrene membranes by electrospinning.* Colloids and Surfaces A: Physicochemical and Engineering Aspects, 2008. **313-314**: p. 411-414.
32. Khenoussi, N., L. Schacher, and D.C. Adolphe, *Nanofiber Production: Study and Development of Electrospinning Device.* Experimental Techniques, 2012. **36**(2): p. 32-39.
33. Lai, C., et al., *Growth of carbon nanostructures on carbonized electrospun nanofibers with palladium nanoparticles.* Nanotechnology, 2008. **19**(19): p. 195303.
34. Lee, H.J. and J.R. Owens, *Motion of liquid droplets on a superhydrophobic oleophobic surface.* Journal of Materials Science, 2010. **46**(1): p. 69-76.
35. Ma, M., et al., *Decorated Electrospun Fibers Exhibiting Superhydrophobicity.* Advanced Materials, 2007. **19**(2): p. 255-259.
36. Ma, M., R.M. Hill, and G.C. Rutledge, *A Review of Recent Results on Superhydrophobic Materials Based on Micro- and Nanofibers.* Journal of Adhesion Science and Technology, 2008. **22**(15): p. 1799-1817.
37. Miyauchi, Y., B. Ding, and S. Shiratori, *Fabrication of a silver-ragwort-leaf-like super-hydrophobic micro/nanoporous fibrous mat surface by electrospinning.* Nanotechnology, 2006. **17**(20): p. 5151-5156.
38. Nuraje, N., et al., *Superhydrophobic electrospun nanofibers.* Journal of Materials Chemistry A, 2013. **1**(6): p. 1929.
39. Park, S.H., et al., *Robust superhydrophobic mats based on electrospun crystalline nanofibers combined with a silane precursor.* ACS Appl Mater Interfaces, 2010. **2**(3): p. 658-62.
40. Sas, I., et al., *Literature review on superhydrophobic self-cleaning surfaces produced by electrospinning*. Journal of Polymer Science Part B: Polymer Physics, 2012. **50**(12): p. 824-845.

41. Srivastava, Y., M. Marquez, and T. Thorsen, *Multijet electrospinning of conducting nanofibers from microfluidic manifolds.* Journal of Applied Polymer Science, 2007. **106**(5): p. 3171-3178.
42. Wang, X., et al., *Large-scale fabrication of two-dimensional spider-web-like gelatin nano-nets via electro-netting.* Colloids Surf B Biointerfaces, 2011. **86**(2): p. 345-52.
43. Wanling Wu, Q.Z., *,‡ Fengling Qing,§ and Charles C. Han*, *<Water Repellency on a Fluorine-Containing Polyurethane Surface.pdf>.* Langmuir, 2009.
44. Xue, C.-H. and J.-Z. Ma, *Long-lived superhydrophobic surfaces.* Journal of Materials Chemistry A, 2013. **1**(13): p. 4146.
45. Zander, N., *Hierarchically Structured Electrospun Fibers.* Polymers, 2013. **5**(1): p. 19-44.
46. Chen, G., et al., *Modification of colloidal silica on the mechanical properties of acrylic based polyurethane/silica composites.* Colloids and Surfaces A: Physicochemical and Engineering Aspects, 2007. **296**(1–3): p. 29-36.
47. PETROVIC, Z.S., *<Structure and Properties of Polyurethane–Silica nanocomposition.pdf>.* Applied Polymer Science, 1999.
48. Kim, J.-Y., S.-B. Shim, and J.-K. Shim, *Synthesis of amphiphilic polyurethane nanonetwork particles and their application for the soil-washing process.* Journal of Applied Polymer Science, 2003. **87**(10): p. 1666-1677.
49. Wang, L., et al., *Fabrication of superhydrophobic TPU film for oil–water separation based on electrospinning route.* Materials Letters, 2011. **65**(5): p. 869-872.
50. Athauda, T.J., P. Hari, and R.R. Ozer, *Tuning Physical and Optical Properties of ZnO Nanowire Arrays Grown on Cotton Fibers.* ACS Appl Mater Interfaces, 2013. **5**(13): p. 6237-46.
51. BARTHLOTT, C.N.a.W., *Characterization and Distribution of Water-repellent, Self-cleaning Plant Surfaces.* 1997. **79**: p. 667–677.
52. Ma, M. and R.M. Hill, *Superhydrophobic surfaces.* Current Opinion in Colloid & Interface Science, 2006. **11**(4): p. 193-202.
53. Cao, Z., et al., *Superhydrophobic pure silver surface with flower-like structures by a facile galvanic exchange reaction with [Ag(NH3)2]OH.* Chem Commun (Camb), 2008(23): p. 2692-4.
54. Jiang, Z.X., L. Geng, and Y.D. Huang, *Design and Fabrication of Hydrophobic Copper Mesh with Striking Loading Capacity and Pressure Resistance.* The Journal of Physical Chemistry C, 2010. **114**(20): p. 9370-9378.
55. Cao, L., H.A. Hu, and D. Gao, *Design and fabrication of micro-textures for inducing a superhydrophobic behavior on hydrophilic*

materials. Langmuir, 2007. **23**(8): p. 4310-4314.
56. Lee, W., et al., *Nanostructuring of a Polymeric Substrate with Well-Defined Nanometer-Scale Topography and Tailored Surface Wettability.* Langmuir, 2004. **20**(18): p. 7665-7669.
57. Tadanaga, K., et al., *Superhydrophobic-Superhydrophilic Micropatterning on Flowerlike Alumina Coating Film by the Sol-Gel Method.* Chemistry of Materials, 2000. **12**(3): p. 590-592.
58. Miyauchi, Y., B. Ding, and S. Shiratori, *Fabrication of a silver-ragwort-leaf-like super-hydrophobic micro/nanoporous fibrous mat surface by electrospinning.* Nanotechnology, 2006. **17**(20): p. 5151.
59. Abdelmegeid1, M.A. and M.Y.S. , *Electrospun Nanofibers with Rough Surface.* JGEB, 2010.
60. Greiner, A. and J.H. Wendorff, *Electrospinning: a fascinating method for the preparation of ultrathin fibers.* Angew Chem Int Ed Engl, 2007. **46**(30): p. 5670-703.
61. Pedicini, A. and R.J. Farris, *Mechanical behavior of electrospun polyurethane.* Polymer, 2003. **44**(22): p. 6857-6862.
62. Bonart, R., *Segmentierte Polyurethane.* Die Angewandte Makromolekulare Chemie, 1977. **58**(1): p. 259-297.
63. Cooper, S.L. and A.V. Tobolsky, *Properties of linear elastomeric polyurethanes.* Journal of Applied Polymer Science, 1966. **10**(12): p. 1837-1844.
64. Mackenzie, J. and E. Bescher, *Structures, Properties and Potential Applications of Ormosils.* Journal of Sol-Gel Science and Technology, 1998. **13**(1-3): p. 371-377.
65. *<fibrillated tencel for battery seperater.pdf>.*
66. Ding, B., et al., *Conversion of an electrospun nanofibrous cellulose acetate mat from a super-hydrophilic to super-hydrophobic surface.* Nanotechnology, 2006. **17**(17): p. 4332-4339.
67. Taepaiboon, P., U. Rungsardthong, and P. Supaphol, *Effect of cross-linking on properties and release characteristics of sodium salicylate-loaded electrospun poly(vinyl alcohol) fibre mats.* Nanotechnology, 2007. **18**(17): p. 175102.
68. Zhang, X.-C., et al., *Thermoplastic polyurethane/silica nanocomposite fibers by electrospinning.* Journal of Polymer Science Part B: Polymer Physics, 2011. **49**(23): p. 1683-1689.
69. Zimmermann, J., S. Seeger, and F.A. Reifler, *Water Shedding Angle: A New Technique to Evaluate the Water-Repellent Properties of Superhydrophobic Surfaces.* Textile Research Journal, 2009. **79**(17): p. 1565-1570.
70. Ashraf, M., et al., *Development of superhydrophilic and superhydrophobic polyester fabric by growing zinc oxide nanorods.* J

Colloid Interface Sci, 2013. **394**: p. 545-53.
71. Pant, H.R., et al., *Photocatalytic TiO2-RGO/nylon-6 spider-wave-like nano-nets via electrospinning and hydrothermal treatment.* Journal of Membrane Science, 2013. **429**: p. 225-234.
72. 李小红, *静电纺纤维膜的疏水性能和拉伸性能的研究.* 2009.
73. 唐超, *聚氨酯/Si02杂纯材料与聚丙烯/聚氨酯/Si02复合材料豹研究.* 2006.
74. Bhushan, B. and Y. Chae Jung, *Wetting study of patterned surfaces for superhydrophobicity.* Ultramicroscopy, 2007. **107**(10-11): p. 1033-1041.
75. Li, D., M.W. Frey, and Y.L. Joo, *Characterization of nanofibrous membranes with capillary flow porometry.* Journal of Membrane Science, 2006. **286**(1-2): p. 104-114.
76. 薛永峰, *静电纺漏斗网蛛蛛丝纳米纤维的制备、表征及其生物相容.* 学位论文, 2007.
77. Xu, B. and Z. Cai, *Fabrication of a superhydrophobic ZnO nanorod array film on cotton fabrics via a wet chemical route and hydrophobic modification.* Applied Surface Science, 2008. **254**(18): p. 5899-5904.
78. Sung Kyoo Park, K.D.K., Hee Taik Kim, *Preparation of silica nanoparticles determination of the optimal synthesis conditions for small and uniform particles.* Colloids and Surfaces A: Physicochemical and Engineering Aspects, 2002. **197**: p. 7-17.
79. Ahn, H.W., C.H. Park, and S.E. Chung, *Waterproof and Breathable Properties of Nanoweb Applied Clothing.* Textile Research Journal, 2011.

초록

투습가능한 초소수성 폴리우레탄/실리카 나노입자 하이브리드 전기방사 나노웹 개발

김소화
의류학 및 의류신소재연구실
서울대학교 대학원

투습성이 우수한 초소수성 나노웹을 제작하기 위하여 전기방사법으로 폴리우레탄/SiO_2 나노파티클(SNPs)을 복합방사하여 표면 거칠기가 증대된 나노웹을 제작하였다. 또한 불소하 처리 없이 DTMS 기상증착으로 표면에너지를 제어하였다.

전기방사용액의 농도를 조절하여 표면구조를 다르게 조절하였으며, 이를 주사초점 현미경으로 관찰하였다. 1~6wt% 농도의 SNPs을 첨가하였을 때 섬유 직경은 평균 600-800nm였으며, SNPs이 나노섬유 표면에 골고루 잘 퍼져 있었다.

순수한 폴리우레탄 나노웹의 접촉각은 131° 였으나, SNPs을 첨가하고 DTMS 의 기상증착 처리를 통해서 PU/SNPs나노웹은 계측적 구조를 이루고 표면에너지가 낮아져 초소수성이 증대된 결과 접촉각이 159° shedding angle이 5°를 보였다. 이것은 나노웹의 표면거칠기가 SNPs로

인해서 증대되고 나노섬유가 다소 두꺼워졌기 때문이다. 한편 표면거칠기가 증대되어도 나노웹의 우수한 투습성은 유지할 수 있었다. 투습성 평가에서 PU/SNPs가 가장 높은 투습성을 보였으며, DTMS 처리 이후에는 다소 감소하였다. 그러나 최종사용 단계에서 나노웹은 직물과 접합하여 사용되고 있으므로 이를 모사하기 위해서 직물에 직접 방사하여 투습성과 공기투과도를 평가하였다. 폴리에스터 직물에 직접 방사하고 CVD 처리한 PU/SNPs 나노웹의 투습량은 6082.3g/m2·24h (ASTM 96 B 염화칼슘법)으로 우수한 투습성을 보였다. 또한 공기투과도는 200cc/sec (below 50 PSI)를 보였다.

주요어: 초소수성, 두습성, 비플루오르화, 전기방사

학번: 2011-23009